The Pennsylvania State University

The Graduate School

Department of Energy and Mineral Engineering

ASSESSMENT OF DELIVERABILITY OF A NATURAL GAS GATHERING AND PRODUCTION SYSTEM: DEVELOPMENT OF AN INTEGRATED RESERVOIR - SURFACE MODEL

A Thesis in

Petroleum and Mineral Engineering

by

Dennis Arun Alexis

Submitted in Partial Fulfillment
of the Requirements
for the Degree of

Master of Science

December 2009

The thesis of Dennis Arun Alexis was reviewed and approved* by the following:

Luis F. Ayala
Assistant Professor of Petroleum and Natural Gas Engineering
Department of Energy and Mineral Engineering
Thesis Advisor

Zuleima T. Karpyn
Assistant Professor of Petroleum and Natural Gas Engineering
Department of Energy and Mineral Engineering

Turgay Ertekin
Professor of Petroleum and Natural Gas Engineering
George E. Trimble Chair in Earth and Mineral Sciences
Undergraduate Program Officer of Petroleum and Natural Gas Engineering
Department of Energy and Mineral Engineering

R. Larry Grayson
Professor of Energy and Mineral Engineering
George H., Jr., and Anna B. Deike Chair in Mining Engineering
Graduate Program Officer of Energy and Mineral Engineering
Department of Energy and Mineral Engineering

*Signatures are on file in the Graduate School

ABSTRACT

Natural gas gathering and distribution systems serve as the primary means to transport gas from the wellhead to the customer. A network designed on sound engineering principles helps to maximize the deliverability from the wells with minimum energy loss during transportation. To achieve this objective, pipeline network models help in characterizing the system to understand the behavior of the network under different operating conditions. In this study, a one dimensional steady state isothermal integrated network model was developed by combining reservoir with surface facility description parameters to effectively capture the variations in flow dynamics with changes in network conditions. In this study, the typical constant supply specification of network analysis was relaxed by implementing gas well deliverability equations at all supply nodes in the system. This model is an extension of the general pipeline network model where the deliverability from the wells are predicted in addition to the nodal pressures in the system based on a set of operating conditions. The model was history matched to the production data from a gas gathering and production system located in Snow Show, Pennsylvania by adjusting the performance constant of the well for a predetermined unique well shut in pressure. With this basic deliverability model in hand, the network was evaluated for several if-then scenarios related to proposed captive modifications to be carried out to analyze the pressure and deliverability changes in the system. Based on the model predictions, recommendations were made to the operator in terms of total production, total sales and fuel consumed by the compressors present in the network. This integrated modeling approach helped in analyzing the system response as a whole and gave a good insight of how the well shut in pressures used in the model had a significant impact on the deliverability predictions.

TABLE OF CONTENTS

LIST OF FIGURES

LIST OF TABLES

NOMENCLATURE

C_p = Pipe Conductivity (MCFD/psi^2)

C_{well} = Well performance constant (MCFD/psi^{2n})

d = Pipe internal diameter (inches)

E_f = Pipe flow efficiency (dimensionless)

f_F = Fanning friction factor

g_c = gravitational constant(ft/s^2)

h_1= Elevation of Pipe at upstream section of pipe (feet)

h_2= Elevation of Pipe at downstream section of pipe (feet)

k_1,k_2,k_3 = Compressor performance constants

L = Length of pipe section (miles)

L_e = Equivalent length of pipe section (miles)

MW_g = Molecular weight of gas (lb/lbmole)

n = Polytropic coefficient (dimensionless)

n_{well} = factor to account for laminar or turbulent flow of gas into the wellbore(dimensionless)

P_{up} = Pressure at upstream section of pipe(psia)

P_{down} = Pressure at downstream section of pipe (psia)

P_{shut} = Shut in pressure at the average reservoir pressure (psia)

P_{wf} = Flowing well face pressure (psia)

P_b = Pressure at base conditions (psia)

P_d = Compressor discharge pressure (psia)

P_s = Compressor suction pressure(psia)

P_{pc} = Pseudocritical pressure (psia)

P_{pr} = Pseudoreduced pressure (dimensionless)

Q_{sc}= Flowrate of gas at standard conditions (MSCFD)

Q = Heat energy added to fluid (Btu)

W = Work done by fluid (Btu)

R = Compression ratio (dimensionless)

s = Pipe elevation adjustment parameter (dimensionless)

T_{av} = Average gas temperature (Rankine)

T_{pc} = Pseudocritical temperature (Rankine)

T_{pr} = Pseudoreduced temperature (Rankine)

U = Internal Energy of fluid (Btu)

Z = Gas compressibility factor (dimensionless)

Z_1 = Gas compressibility at compressor suction conditions (dimensionless)

GREEK

α = Number of stages in a compressor

ρ = Gas density (lb/ft^3)

μ_g = Gas viscosity (centipoise)

γ_g = Gas specific gravity (dimensionless)

η = Operating efficiency of the compressor (dimensionless)

ACKNOWLEDGEMENTS

I would like to express my gratitude to the Department of Energy and Mineral Engineering for having accepted me to pursue my graduate study at Penn State. My advisor, Dr. Luis Ayala and Dr. Zuleima Karpyn have always been there to help, support and guide me throughout my entire period of study at Penn State. If I am a more refined and knowledgeable person today it is because of them.

I would also like to thank Dr. Turgay Ertekin for graciously accepting to be in my thesis committee and I feel it is a great honor.

I would also like to thank Dr. Joel Haight for giving me his invaluable views at different times both for life and profession.

I am always grateful and indebted to my friends at Penn State, my parents, grandmother and family members and friends in India for providing me the strength and encouragement at all times which helped me to stay focused and dedicated.

Finally a big word of thanks and appreciation goes to the managing partners of NCL Natural Resources, LLC for providing me the much needed financial support to successfully complete my research.

Chapter 1

INTRODUCTION

In the United States, interstate and intrastate gas pipelines are the main source for transporting natural gas from the reservoir to its point of demand. The total pipe mileage of the natural gas distribution network in the U.S. is 305,000 miles (US DOE, accessed June 2009). The steady increase in the exploration of natural gas over the recent years has prompted operators to re evaluate the performance of the existing pipeline infrastructure to accommodate additional new volumes brought into the system. Natural gas gathering systems which collects gas from the wells and feeds to the main trunk or the distribution line has to be efficiently designed or modified such that maximum amount of gas is drawn out of the reservoir with minimum energy losses.

A design or a modification of a gas network requires a sound understanding of the flow dynamics that is expected to happen once the network is operational. Gas network models which are widely used in the gas transmission industry help to achieve this objective by completely characterizing the network under analysis. These models are built on the fundamental principles of thermodynamics of fluid flow in pipes. Models have a high degree of flexibility, repeatability and modeling consumes less time. Predicting the total volume output of a network (that is the capacity) under analysis forms a major part of the modeling process. The total gas deliverability from a network is affected by pressure changes caused by new volume additions or pipe layout changes etc. Deliverability from the network can also be affected by unaccounted gas losses such as pipe leaks, error in gas volume measurement at the wellheads. Compressors present in a network also utilize some gas for operation which should also be accounted when computing the total volume of gas that is eventually distributed or sold.

In this work, a pipeline network model was developed to predict the production performance of a network with changes in network pressure at steady state and isothermal conditions. To meet this objective the gas well deliverability equation was employed to build the integrated model. This

model computes the amount of gas flowing out of each well in a network when the shut in pressure and the well performance constant are provided as inputs in addition to simulating the nodal pressures.

Production data collected from a gas field operating in Pennsylvania was used to validate the developed model. In addition, good history matches indicated the model's adaptation to the gas field and operating conditions. As a further step this customized model was used as a diagnostic tool to evaluate several if-then scenarios for estimating the total gas volume output from the given network. This model can also be used as a valuable tool for identifying how the network could behave when modifications such as realignment of pipe layout, addition of new volumes that may be carried out in the existing network. The results of the model will provide a handle for evaluating the economics of implementing such changes in future studies.

Chapter 2

BACKGROUND

Integrated gas network models which combine surface/ subsurface parameters to characterize a gas gathering system and the hydrocarbon formation as one interacting entity were developed to aid better planning and management of the reservoir in terms of forecasting, field development and analysis of surface infrastructure expansion. Such models help to forecast the capital investment needed at the various stages in the life of a reservoir as many number of wells would be tied in to the existing surface transportation network during the expansion phase. Models can be integrated by combining a numerical reservoir simulator with a conventional surface pipe network simulator (Startzman *et al.* 1977) where data is exchanged to compute flow and nodal pressure depending on the boundary conditions imposed. Successful predictions from these models primarily rely on the amount of information provided as inputs to them. Integrated models significantly help to design surface gathering and processing facilities especially during the initial field development. However a mature field having inadequate reservoir information can pose as a significant challenge during its expansion phase as field deliverability can be greatly affected by improper design and sizing of surface facilities. Developing a simple reliable model becomes a necessity during the prediction of field deliverability from mature fields when minimum known reservoir parameters are available and the use of full scale reservoir simulator is not possible.

Stoner (1969) proposed a method that for the first time combined pipelines, gas storage fields, compressors into a single integrated system and solve for the different parameters associated with different facilities by using the Newton – Raphson numerical solution technique assuming steady state flow conditions. His method essentially defined the various surface facilities and subsurface systems by using their respective design equations to represent them as a function of gas flow rate in the model and solve them by using the conventional nodal analysis technique.

Baldwin (1980) proposed a method of using a pseudo back pressure curve considering the gas reservoir to be one large well to determine the gas deliverability depending on various compression requirements by a compressor gathering gas was for an offshore gas field in the Gulf of Mexico.

Puchyr (1991) discusses about the development of an integrated model which combines a gas reservoir simulator with the surface network model assuming single phase fluid flow in the surface pipelines. The surface network model calculated the flow rate by using the static reservoir pressure. A polynomial equation was used by the network simulator to model the pressure losses in wellbore and pipelines. This flow rate would be passed to the reservoir simulator and the iterations would be continued till the flowing bottom hole pressures calculated by the reservoir simulator and the network simulator matched within a specified convergence tolerance criteria.

Mogensen *et al.* (1995) discuss about an integrated model which was first developed for the Sexsmith gas field in Alberta, Canada by combining a three dimensional black oil simulator called ECLIPSE and a pipeline network simulator FORGAS. This interfaced model had the capability to simultaneously exchange flow and pressure information at each iteration level. The pressures and flow rates are exchanged back and forth between the two simulators till the difference between the well flow rates used by the pipeline simulator at current iteration and the previous iteration is less than the specified tolerance level based on the bottom hole pressure calculated by the pipe simulator which is used by the reservoir model to compute the flow rates to be provided as input to the pipe simulator. This model had also the flexibility to model different types of reservoirs and was more stable when capturing transient flow behavior.

A simulation technique involving a pipe network simulator NETOPT and a reservoir simulator ECLIPSE was described by Hepguler and Dutta–Roy (1997). The numerical simulator generates the inflow performance relationship for each well and transfers the information to the pipe network simulator and the flow rate and pressure convergence during each time step is done before proceeding to the next time step thereby avoiding a generalized inflow performance relationship (IPR) curve. Also the changes in gas oil ratio (GOR) and water production are captured in this model.

Litvek *et al*. (1997) describes a model especially designed for modeling the Prudhoe Bay field. In this model the well face flowing pressures were computed by the network simulator and passed on to the reservoir simulator to get the flow rate from the wells, fluid saturations and compositions.

Tingas *et al*. (1998) describe a coupled simulation package to model different gas reservoirs present in the North sea producing at different stages of depletion tied to the same surface transportation network. The pipe network simulator was PIPEPHASE and the three dimensional reservoir simulator used was GCOMP. This model helped in better reservoir management where many wells streams combine together and the net production from the field is constrained by the existing surface infrastructure. The three primary calculations carried out in this model are the flow and pressure changes in the reservoir, the pressure drop in the production tubing and the pressure drop in the surface pipeline network respectively.

An integrated surface/ subsurface model were described by Holst *et al.* (1999) for modeling the flow of a single phase fluid from a tight gas formation. This model was developed to optimize the entire surface network when new additional wells were being tied in the existing network. The surface network model solves for the well production flow rates. These flow rates are used by the

reservoir model to pressure distribution in the formation. The back pressure equation was used by the reservoir model to come up with well deliverabilities. The well deliverability coefficient "C_{well}" in the model was calibrated based on a match between wellhead pressure calculated by the reservoir model and the surface network model. In a similar fashion the surface facilities were calibrated by tuning the flow efficiency of the pipes. Corrections to account for water flow in the wellbore were also incorporated in the model.

Marsh and Kenny (2002) discuss about the complete development of a low permeability, under pressured gas field starting from drilling to gas delivery with the help of an integrated model which effectively portrayed the interaction between the reservoir and surface transportation facilities for multiphase flow in pipes. The model uses the backpressure equation (Rawlins and Schellardt, 1936) to quantify the well deliverability. The well deliverability constant "C_{well}" in this equation was calculated on a well by well basis by using well test and production data. The average reservoir pressure was computed using the material balance equation utilizing the original gas in place (OGIP) and the cumulative gas produced. The flowing bottom hole pressure was calculated as a function of well head pressure and the pressure drop in the tubing string.

Stevenson and O'Shea (2006) describe an integrated model which was useful in the expansion of a tight gas gathering system located in Western Colorado. The model is a combination of a reservoir model and a pipeline model. The reservoir model predicts the deliverability curve for each producing well using the Rawlins – Schellardt (1936) back pressure equation for the current operating conditions. This model had the capability to forecast future pipeline infrastructure and compression requirements based on the anticipated drilling activity.

Krishnamurthy (2008) describes about a steady state single phase gas flow model developed specifically to characterize a gas gathering system in Pennsylvania. The model had the capability

to compute the compression requirements, pressure drop and gas flow in pipe sections in addition to simulating the nodal pressures for the given flow rate specifications based on a given set of operating conditions. To capture the non idealities in the system due to the presence of water, the individual pipe flow efficiencies of pipes in the network was tuned based on an optimization procedure described. The entire network was screened and pipe sections having poor flow efficiencies and high pressure drop were reported.

Aina,I (2006) studied the flow of natural gas in pipelines both under steady state and transient flow conditions. Unsteady flow which is the flow of gas in pipelines in reality was modeled by modifying the procedure proposed by Wylie *et al. (*1971) for modeling transients in gas pipelines. Computation time required to solve the node continuity equations was decreased by eliminating iteration required at every time step and also by making use of an inertial multiplier in the finite difference approximation of the momentum equation.

Carrillo (1999) developed a model to address the phenomenon of two phase flow to understand the behavior of natural gas transmission networks under a wide variety of operating conditions. The hydrodynamic model developed essentially integrated the phase behavior prediction tool to predict the phase properties and the double stream model to track the splitting of phases in T junctions of the network. The model developed was an extension of the previous simulator built by Martinez (1994).

Nagoo (2003) developed a single phase, isothermal and quasi steady state model for integrating valves, regulators, compressors present in a natural gas transportation network. This model essentially captured the slow transients in a pipe network. To model the complexity of a gas network with respect to topology a Topologically Sorted Spanning Tree (TSST) technique is used

in the model. This technique helped to accommodate the facilities in the network regardless of their size or complexity.

Chapter 3

PROBLEM STATEMENT

The infrastructure of a gas transportation network erected for conveying gas from the reservoir to its point of demand can change as the field is developed with projected drilling activity. Whenever modifications are carried out to an existing gas network, the existing stabilized pressure and flow regime changes. Gas network models built to simulate pressures at various nodes in the system for the given production flow rates are helpful in identifying sections in the pipe having poor pipe flow efficiencies resulting in major energy loss. These models cannot effectively characterize the associated change in well deliverability as they simulate based on the assumption that the production from the wells will be the same although the system pressure changes.

In this study, an integrated gas network model is developed to capture the associated flow changes in the system whenever the network pressure changed. This is done by incorporating the reservoir description parameters into the surface pipeline network model by making use of the gas well deliverability equation. The subsurface properties are incorporated into the model by three parameters namely well shut in pressure, well performance constant and the non ideality factor to describe the laminar/ turbulent nature of flow into the wellbore. An integrated model like the one developed can be used for a comprehensive analysis of a gas network system to predict the accompanying flow changes due to the system pressure variation whenever a new well addition or pipeline expansion is done. The significance of such a model is its capability to predict the flow and pressure changes in the gas network and decide on the physical feasibility of the proposed modifications and guide the operators on the capital investment needed in such expansions.

Chapter 4

MODEL DESCRIPTION

The main governing equations used in this integrated model are the pipe performance equation, the well deliverability equation and the node continuity equations. The gas network has to be characterized first to generate the associated pipe, reservoir and fluid properties. Number of pipes, number of nodes, number of compressors, pipe properties, fluid properties, well shut in pressure, well performance constant and the non ideality factor for each producing well has to be provided as inputs to the model.

In addition to the above inputs the model has the capability to use four different types of pipe flow equations for computing the upstream and the downstream pressures in a pipe. They are the general pipe flow equation or Weymouth, Panhandle A and Panhandle B based on the different friction factor model built into them. The compressors present in a network are characterized by the theoretical compressor equation as shown in Appendix A. The compressor is modeled based on the suction, discharge or the HP required for compression. The flow of gas from every producing well in the network is modeled using the gas well deliverability equation based on the shut in pressure, well performance constant and the non ideality factor. The model is further enhanced by its capability to account for the gas consumption by a compressor in the network. This is estimated by the user specification of the amount of fuel consumed per unit of brake horse power output. The model also accounts for the wellhead gas losses when a gas loss fraction factor is specified as input.

4.1 Gas Network Modeling

A gas network is comprised of nodes and node connecting elements. The nodes can be the junction points between two node connecting elements or the well heads which are supplying gas into the network or a demand point where gas is being sold. The node connecting elements can be pipe legs, compressors, valves or regulators present in the network to build a continuous flow path between the supply and the demand points. Figure 4-1 shows a simple gas transportation network describing the nodes and the node connecting elements.

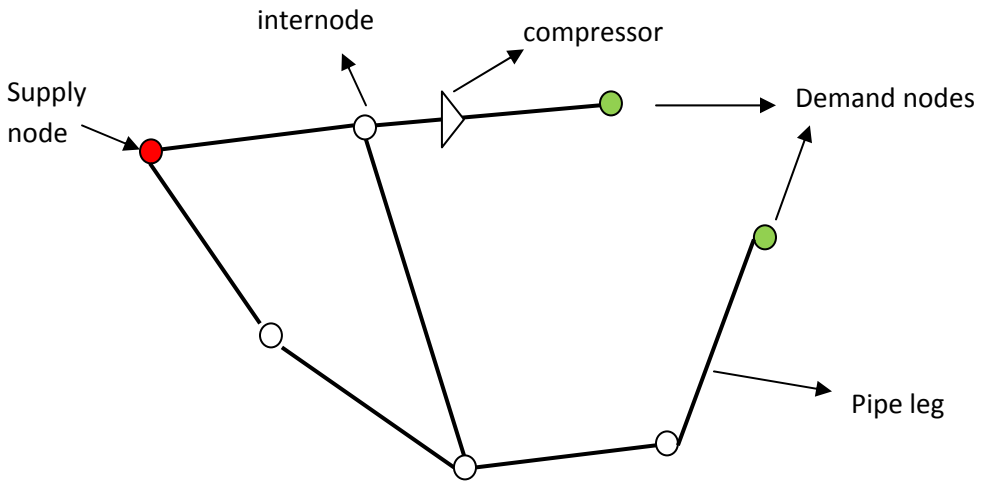

Figure 4-1: A simple gas transportation network to illustrate nodes and node connecting elements

In Figure 4-1 the nodes are represented by circles. The red color node is a supply node which is a point in the network where gas is supplied into the network. This node can also be the point where gas from a well enters the network. The green color nodes represent the demand nodes where the gas which entered at the supply node leaves the network. The white nodes represent the internodes which connect two node connecting elements to serve as a link between the node connecting elements to make a continuous flow path for conveying the gas. The node connecting elements are the pipes and the compressor which are represented by black colored lines and the triangle respectively.

Modeling a gas network is done by integrating the nodes and the node connecting elements by using appropriate design equations for them. In this steady state model developed, the equations used for the node connecting elements are for the pipe and the compressor and the supply nodes are characterized by the well deliverability equation. These equations primarily relate the volume of fluid transmitted through the facilities or volume produced from the wells to various factors and are linked by constructing the node continuity equations for every node which ensures that mass is conserved at every single node in the system. These node continuity equations are solved simultaneously to solve for the pressures at every node based on a given set of boundary conditions. The node continuity equations can be constructed either in the P formulation or the Q formulation methodology. In the P formulation technique, the unknowns are the pressures at various nodes in the system and in the Q formulation technique the unknowns are the flows across the facilities (node connecting elements) in the system. With the pressure simulated, the flow can be computed or the vice versa. The P formulation and the Q formulation techniques are discussed later. The next three sections describe the design equations used for modeling the pipe, compressor and the well.

4.2 One dimensional steady state Gas flow equation in Pipes

This model is built based on the assumption that the amount of gas flowing in any section of the pipe in the network is at steady state conditions and there is no generation or accumulation of mass at any point in the network and the temperature of the gas remains practically unchanged. Consider a horizontal pipe section shown in Figure 4-2. Writing a thermodynamic balance by invoking the 1^{st} and 2^{nd} laws of thermodynamics at the inlet and the outlet of the pipe at steady state we get the Bernoulli's energy balance equation as

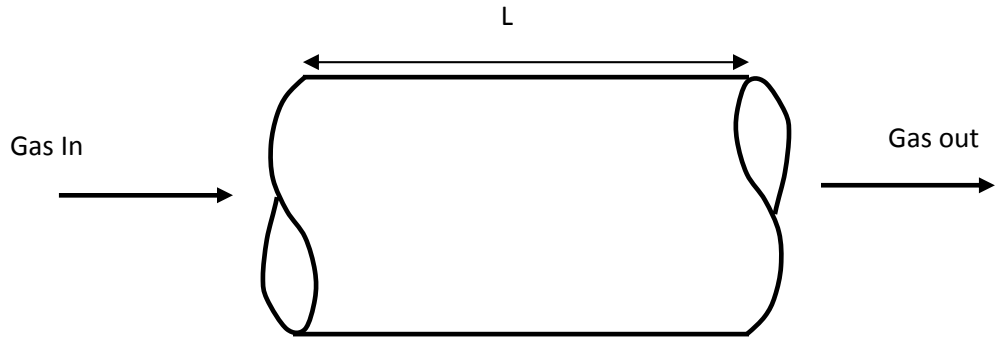

Figure 4-2: Illustration of a single phase gas flow through a pipe section

$$\frac{dP}{\rho} + \frac{vdv}{g_c} + \frac{gdz}{g_c} + \delta(\text{losses}) = 0 \quad \text{----(4.1)}$$

where,

$\frac{dP}{\rho}$: Pressure energy term

$\frac{gdz}{g_c}$: Potential Energy term

$\frac{vdv}{g_c}$: Kinetic energy term

$\delta(\text{losses})$: losses due to irreversibilities in the process

Equation 4.1 can be rewritten in the form of pressure gradient as follows

$$\frac{dP}{dx_{(\text{total})}} = \frac{dP}{dx_{(\text{friction})}} + \frac{dP}{dx_{(\text{elevation})}} + \frac{dP}{dx_{(\text{accelaration})}} \quad \text{---- (4.2)}$$

In equation 4.2, $\frac{dp}{dx_{(\text{friction})}}$ term replaces the $\delta(\text{losses})$ term in equation 4.1 and is a function of friction factor for straight pipes and defined as

$$\frac{dP}{dx_{(\text{friction})}} = -\frac{2\rho v^2 f_F}{g_c d} \quad \text{---- (4.3)}$$

If the same pipe section shown in Figure 4-2 is inclined at an angle θ to the horizontal as shown in Figure 4-3 then the pressure change due to elevation can be defined as

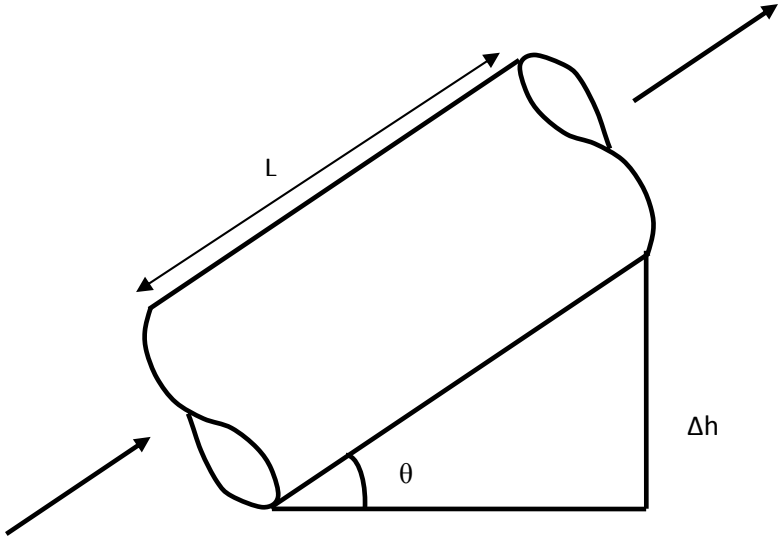

Figure 4-3: Illustration of a single phase gas flow through a pipe section inclined at an angle θ

$$\frac{dP}{dx_{(elevation)}} = -\frac{\rho g}{g_c}\sin\theta = -\frac{\rho g \Delta h}{g_c L} \quad \text{---- (4.4)}$$

where,

ρ = Gas density (lbm/ft^3)

v = Gas velocity (ft/s^2)

p = Pressure (psia)

g = Acceleration due to gravity (ft/s^2)

g_c = Factor for unit conversion (lbm ft/lbf s^2)

The contribution of $\frac{dp}{dx_{(accelaration)}}$ is usually neglected when compared to the influence of the rest of the terms in equation 4.2, thus

$$\frac{dP}{dx_{(total)}} = \frac{dP}{dx_{(friction)}} + \frac{dP}{dx_{(elevation)}} \quad \text{---- (4.5)}$$

or

$$\frac{dP}{dx_{(total)}} = -\frac{\rho g \Delta h}{g_c L} - \frac{2\rho v^2 f_F}{g_c d} \quad \text{---- (4.6)}$$

Using the definitions of velocity and area as shown in equations 4.7 and 4.8 and using them in equation 4.6 we get equation 4.9

$$v = \dot{m}/\rho a \text{ ---- (4.7)}$$

$$A = \pi d^2/4 \text{ ---- (4.8)}$$

$$\frac{dP}{dx_{(total)}} = -\frac{\rho g \Delta h}{g_c L} - \frac{32\dot{m}^2 f_F}{\pi^2 g_c \rho d^5} \text{ ----- (4.9)}$$

or

$$\frac{\rho dP}{dx_{(total)}} = -\frac{\rho^2 g \Delta h}{g_c L} - \frac{32\dot{m}^2 f_F}{\pi^2 g_c d^5} \text{ ---- (4.10)}$$

Separating the variables in equation 4.10 we get equation 4.11

$$\rho dP = - \left(\frac{\rho^2 g \Delta h}{g_c L} + \frac{32\dot{m}^2 f_F}{\pi^2 g_c d^5}\right) dx \text{ ---- (4.11)}$$

Density of gas can be defined as

$$\rho = \frac{\gamma_g P Mwair}{T_{av} Z_{av} R} \text{ --- (4.12)}$$

where:

γ_g = Gas gravity (dimensionless),

Mwair = Molecular weight of air (lb/lbmole),

Tav = Average temperature of gas (R),

Zav = Average Z factor of gas (dimensionless),

R = Universal gas constant (psia.ft^3/lbmole.R),

Using density of the gas, ρ at average conditions as defined by equation 4.12 in equation 4.11 we get equation 4.13

$$-\int_{P_1}^{P_2} \left\{ \frac{\frac{P\, Mwair\, \gamma_g}{T_{av} Z_{av} R}}{\frac{P^2\, Mwair^2\, \gamma_g^2\, g\, \Delta h}{T_{av}^2\, Z_{av}^2\, R^2\, g_c\, L} + \frac{32\dot{m}^2 f_F}{\pi^2 g_c d^5}} \right\} dP = \int_0^L dx \text{ ---- (4.13)}$$

Integrating equation 4.13 one obtains,

$$\frac{T_{av}Z_{av}\ R\ g_c L}{g\ Mwair\ \Delta h\ \gamma_g\ ^2}\ \ln\left\{\frac{P_1{}^2\ Mwair^2\ \gamma_g{}^2\ g\ \Delta h}{T_{av}{}^2\ Z^2{}_{av}\ R^2\ g_c\ L}+\frac{32\dot{m}^2 f_F}{\pi^2 g_c d^5}\right\}=\ \text{L --- (4.14)}$$

or

$$\ln\left\{\frac{P_1{}^2\ Mwair^2\ \gamma_g{}^2\ g\ \Delta h}{T_{av}{}^2\ Z^2{}_{av}\ R^2\ g_c\ L}+\frac{32\dot{m}^2 f_F}{\pi^2 g_c d^5}\right\}=\ \frac{2\ \Delta h\ g\ Mwair\ \gamma_g}{T_{av}Z_{av}\ R\ g_c}\ \text{---- (4.15)}$$

$$\text{By letting}\quad s=\frac{2\ \Delta h\ g\ Mwair\ \gamma_g}{T_{av}Z_{av}\ R\ g_c}\ \text{---- (4.16)}$$

Equation 4.15 becomes

$$\ln\left\{\frac{P_1{}^2+\frac{T_{av}{}^2\ Z^2{}_{av}\ R^2\ g_c\ L\ 32\dot{m}^2 f_F}{Mwair^2\ \gamma_g{}^2\ g\ \Delta h\ \pi^2 g_c d^5}}{P_2{}^2+\frac{T_{av}{}^2\ Z^2{}_{av}\ R^2\ g_c\ L\ 32\dot{m}^2 f_F}{Mwair^2\ \gamma_g{}^2\ g\ \Delta h\ \pi^2 g_c d^5}}\right\}=\quad s\ \text{----- (4.17)}$$

Taking antilog of equation 4.17 one gets

$$P_1{}^2+\frac{T_{av}{}^2\ Z^2{}_{av}\ R^2\ g_c\ L\ 32\dot{m}^2 f_F}{Mwair^2\ \gamma_g{}^2\ g\ \Delta h\ \pi^2 g_c d^5}=\frac{T_{av}{}^2\ Z^2{}_{av}\ R^2\ g_c\ L\ 32\dot{m}^2 f_F}{Mwair^2\ \gamma_g{}^2\ g\ \Delta h\ \pi^2 g_c d^5}e^s+P_2{}^2\ e^s\ \text{----- (4.18)}$$

or

$$P_1{}^2-\ e^s P_2{}^2=\frac{T_{av}{}^2\ Z^2{}_{av}\ R^2\ g_c\ L\ 32\dot{m}^2 f_F}{Mwair^2\ \gamma_g{}^2\ g\ \Delta h\ \pi^2 g_c d^5}(e^s-1)\qquad\text{----- (4.19)}$$

Multiplying and dividing by s in the right hand side of equation 4.19 it becomes,

$$P_1{}^2-\ e^s P_2{}^2=\frac{64\dot{m}^2 f_F\ \ T_{av}Z_{av}\ R}{\pi^2 g_c d^5\ Mwair\ \gamma_g}L_e\ \text{---- (4.20)}$$

where:

$$L_e=L(e^s-1)/s\ \text{---- (4.21)}$$

Now separating the mass flowrate $\dot{m}^2$ term from rest of the terms in equation 4.20 becomes

$$\dot{m}^2 = \frac{(P_1{}^2 - e^s P_2{}^2)\pi^2 g_c d^5 \text{Mwair}\,\gamma_g}{64 f_F\ \text{T}_{av}\text{Z}_{av}\ \text{R Le}} \quad \text{----- (4.22)}$$

We know that $\dot{m} = \rho_{sc} q_{sc}$ ----- (4.23)

Therefore equation 4.22 becomes

$$\text{q}_{sc} = \left(\frac{\text{T}_{SC}}{\text{P}_{SC}}\right)\sqrt{\frac{\text{g}_c\pi^2\text{R}}{64\text{Mwair}}}\sqrt{\frac{1}{\text{f}_F}}\sqrt{\frac{\text{P}_{up}{}^2 - \text{e}^s\text{P}_{down}{}^2}{\text{T}_{av}\text{Z}_{av}\ \text{Le}\,\gamma_g}}\ \text{d}^{2.5} \text{ ---- (4.24)}$$

To make the units of volumetric flow rate to be in SCFD, unit conversion is done in equation 4.24 to yield equation 4.25 which is the general one dimensional steady state isothermal pipe flow equation.

$$\text{q}_{sc} = 38.774\left(\frac{\text{T}_{SC}}{\text{P}_{SC}}\right)\sqrt{\frac{1}{\text{f}_F}}\sqrt{\frac{\text{P}_{up}{}^2 - \text{e}^s\text{P}_{down}{}^2}{\text{T}_{av}\text{Z}_{av}\ \text{Le}\,\gamma_g}}\ \text{d}^{2.5} \text{ ---- (4.25)}$$

where:

T_{sc} = Temperature at standard conditions,

P_{sc} = Pressure at standard conditions,

f_F = Fanning friction factor (dimensionless),

d= Internal diameter of the pipe (inches),

P_{up} = Pressure at the upstream end of the pipe (psia),

P_{down} = Pressure at the downstream end of the pipe (psia),

T_{av} = Average temperature of flowing fluid in pipe (R),

Z_{av} = Average compressibility factor of the flowing gas (dimensionless),

γ_g = Fluid specific gravity (dimensionless),

s =Elevation adjustment parameter (dimensionless),

L_e = Equivalent length of the pipe section (miles)

The equivalent length of the pipe, L_e can be defined as shown in equation 4.21. Equation 4.21 is valid for a pipe having a uniform slope. The L_e for pipe sections having non uniform slope is defined as shown in equation 4.26

$$L_e = L_1(e^{s_1} -1)/s_1 + L_2e^{s_1} (e^{s_2} -1)/s_2 + L_3e^{s_1+s_2} (e^{s_3} -1)/s_3 + \ldots\ldots. L_ne^{\sum s_{n-1}} (e^{s_n} -1)/s_n \text{ ----- (4.26)}$$

where:

n = Number of slopes present in the pipe section (dimensionless)

Equation 4.25 represents the theoretical flow rate of the gas flowing through the pipe section if the pipe section was 100% efficient to transmit the flowing gas. In reality the flowrate of the gas flowing through a pipe section is always less than the maximum theoretical flow rate. This is due to the presence of water, condensate or oil in the line. The actual flow rate of gas is obtained by multiplying the theoretical flow rate with a factor called the flow efficiency, E_f . The definition of E_f is given in equation 4.27

$$E_f = \frac{q_{sc_{actual}}}{q_{sc_{theoretical}}} \text{ ---- (4.27)}$$

Therefore equation 4.25 can be modified by including the flow efficiency factor, E_f to get the actual flow rate as shown in equation 4.28

$$q_{sc_{actual}} = 38.774 \left(\frac{T_{SC}}{P_{SC}}\right) \sqrt{\frac{1}{f_F}} \sqrt{\frac{P_{up}^2 - e^s P_{down}^2}{T_{av} Z_{av} \; Le \, \gamma_g}} d^{2.5} E_f \text{ ----- (4.28)}$$

Equation 4.28 can also be expressed as shown in equation 4.29

$$q_{sc_{actual}} = C_P (P_{up}^2 - e^s P_{down}^2)^{\frac{1}{n}} \text{----- (4.29)}$$

where:

$$C_p = 38.774E_f\,(T_{sc}/P_{sc})(1/f_F)^{0.5}\,(1/\gamma_g T_{av} Z_{av} L_e)^{0.5} d^{2.5} \text{ ------ } (4.30)$$

The C_p in equation 4.29 is the pipe conductivity which is a function of fluid, pipe properties, friction factor and the flow efficiency. The flow efficiency is parameter unique to each pipe which when multiplied by the predicted flow rate gives the actual flow rate present in the pipe. The flow efficiency captures the non idealities which are not captured by the friction factor. Equation 4.29 is used in the model and different flow equations were developed based on the definition of friction factor incorporated in equation 4.29. The equations which are used in the model are the General flow equation with rigorous friction factor, Weymouth, Panhandle A and Panhandle B. As described before, the model has the capability to use any of the four flow equations as specified by the user. These flow equations with their respective friction factor definitions are described in Appendix B.

4.3 Compressor Modeling Equation

Compressors are an integral part of any gas transportation network. They primarily serve three purposes. To gather gas from any location in the network, to increase the pressure of the transported gas to feed the gas to a main pipeline network and to increase the deliverability from the wells at the given operating conditions by lowering the well head pressures. There are three types of compression process. They are the isothermal, isentropic and the polytropic compression process. Compressor equations are developed based on the assumption that the compressed fluid undergoes an isentropic behavior. The power required for compression is essentially the work done on unit mass of fluid to raise the pressure to a desired value under steady state conditions. In the normal compression process, non isentropic conditions are represented by including the polytropic coefficient ‘n’ instead of the isentropic coefficient ‘k’ as there will be some energy

loss or gain in the actual compression. Equation 4.31 represents the standard compressor performance equation used in the industry. The development of equation 4.31 is shown in Appendix A.

$$\frac{HP}{Q_s} = (k_1 R^{k_3} - k_2) \text{ -------} \quad (4.31)$$

where:

HP = Compression horse power,

R = Compression ratio (dimensionless),

Qs = Gas flow rate through the compressor (MMSCFD),

$k_1 = k_2 = (3.03P_{sc}/\eta)\alpha(n/(n-1))(Z_1/Z_{sc})(T_{av}/T_{sc})$ ----- (4.32),

$k_3 = (n - 1)/\alpha n$ ------ (4.33),

Psc = Pressure at standard conditions (psia),

Zsc = Compressibility factor of the fluid at standard conditions (dimensionless),

Z_1 = Compressibility factor at suction conditions (dimensionless),

η = Operating efficiency of the compressor (dimensionless),

α = Number of stages of compression (dimensionless),

Tav = Average temperature of the fluid (R),

Tsc = Temperature at standard conditions (R),

n = Polytropic coefficient (dimensionless)

k_1, k_2, k_3 represent the compressor performance constants and are usually specified by the manufacturer. In this model, equation 4.31 is used for predicting the horse power requirements when the compressor performance constants and the suction or discharge pressure are specified as inputs. The model has the option to specify the HP or suction pressure or the discharge to predict the other two variables.

4.3.1 Accounting Compressor Fuel Consumption

In normal operation of a gas network system, some of the transported gas is used for operation of the compressors in the network. Though the total fuel consumption of the compressors is much less when compared to the total amount of gas transported, accounting gas fuel consumption in the modeling process will help us to determine how much gas is used for the compressor operation. This can indicate whether the compressors are correctly sized to perform the required compression process. The rate of fuel consumed by a compressor is normally reported as the cubic feet of gas consumed in one hour for producing one hp of work output and represented as "cf/BHP – hr". If the "cf/BHP – hr" for a compressor is known, then the total fuel consumed by that compressor can be calculated. This volume of gas consumed as fuel is essentially subtracted from the volume of gas which appears at the compressor suction to account for the gas consumption as fuel. The efficiency of the compressor is one of the important factors which determine the total HP required for compression which in turn determines the fuel required. The compressor performance constants k_1 and k_2 as defined by equations 4.32 and 4.33 shows that they are a function of compression efficiency and the HP required changes when k_1 and k_2 change. As the efficiency of the compressor increases the fuel required becomes less for the same amount of compression performance.

4.4 Gas Well Modeling Equation

The gas well deliverability equation is employed to model the gas supply nodes in the network which are treated as wells in this model. The relationship representing the flow of gas into the wellbore from the formation is shown in equation 4.34 (Kelkar, 2008)

$$q_{sc} = C_{well}(P_{shut}^{2} - P_{wh}^{2})^{nwell} \text{ ----- (4.34)}$$

where:

q_{sc} = Gas production flow rate (MCFD),

C_{well}= Performance constant for the well (MCFD/psi^{2nwell}),

P_{shut} = Shut in well head pressure of the well at the average reservoir pressure (psia),

P_{wh} =Flowing well head pressure (psia),

n_{well} = Factor to account for the non ideal flow behavior of gas into the wellbore

The performance constant 'C_{well}' of the well is a function of reservoir and fluid properties. The factor 'n_{well}' to characterize non ideal flow behavior varies between 0.5 – 1.0, with 1 representing completely turbulent flow and 0.5 representing laminar flow. The production from a gas well is often dependant on various conditions of wellhead pressure, sand face pressure and the reservoir pressure. The gas well which is normally connected to a surface pipeline network, flows depending on the operating pressure of the pipeline in the system. The backpressure prevailing at the wellheads is more often the one which affects the sand face pressure to determine the amount of gas flowing into the wellbore. Equation 4.34 is used in the model to predict the supply flow rate from a well for the existing pressure at the wellhead which is the nodal pressure calculated at that particular supply node by the model.

4.5 Accounting Well Head Losses

In a gas transportation network system, based on operational experience, the quantity of gas which eventually reaches the sales is different from the quantity of gas which is actually produced. The reason for such discrepancy can be due to error in recording or measuring the exact quantity of gas at the well head or it can be due to the presence of leaks in the facilities present in the infrastructure of the gas network system. Though these sources of error are difficult to exactly quantify, an empirical quantification can be done. In this model to account for such

losses in the system, a factor called the 'Gas Loss Factor' can be specified as one of the inputs to the model. This factor is basically a fraction (0.0 – 0.5) and when specified, the model uniformly subtracts this fraction from all the predicted flow rates at the well nodes. The remaining quantity of gas is assumed to flow through the network to reach the sales after accounting for gas consumed as fuel by the compressors.

4.6 Fluid Properties

The properties of the gas which are required as inputs to the model are the critical properties, compressibility factor, specific gravity and gas viscosity.

Specific gravity

The specific gravity (γ_g) of a natural gas is the defined as the ratio of the molecular weight of the natural gas to the molecular weight of air as defined in equation 4.35. The molecular weight of air is normally taken as 28.97 lbm/lbmole. If the natural gas stream is very lean that is it is primarily composed of methane then equation 4.35 can be used to calculate the specific gravity of the gas. If on the other hand the natural gas stream is a mixture of ethane, propane etc., then the apparent molecular weight of the gas stream must be used in equation 4.35 to compute the specific gravity.

$$\gamma_g = \text{Molecular weight of natural gas stream / Molecular weight of air} \quad \text{----- (4.35)}$$

where:

$\boldsymbol{\gamma_g}$ = Gas gravity (dimensionless)

The apparent molecular weight of a natural gas stream is the sum of the product of individual molecular weights of the components and their respective compositions in the stream. A gas reservoir which has primarily methane would have a specific gravity of 0.55. A rich gas

formation can have a specific gravity in the range of 0.75 – 0.9. In this model the specific gravity has to be directly given as one of the inputs and this will be used to primarily calculate C_p (pipe conductivity). In addition to this the gas gravity is also used for calculation of the critical temperature and pressure.

Critical Properties

With the specific gravity of the gas stream known, the pseudo critical temperature (T_{pc}) and the pseudo critical pressure (P_{pc}) can be calculated using the correlation described in equations 4.36 and 4.37. The correlations are valid $H_2S < 3\%$, $N_2 < 5\%$ and total inorganic content < 7%.

$$Ppc = 709.604 – 58.718\ \gamma_g \text{ ------ (4.36)}$$

$$Tpc = 170.491 + 307.344\ \gamma_g \text{ ------ (4.37)}$$

where:

Ppc = Pseudo critical pressure (psia),

Tpc = Pseudo critical temperature (R),

γ_g = Gas gravity (dimensionless)

Compressibility factor

Gases are fluids which are highly compressible in nature. The volume changes associated with pressure changes at a given temperature is accounted by the compressibility factor or the Z factor. The Z factor is defined as the ratio of gas volume to the volume occupied by the same gas if it were an ideal gas at the given pressure and temperature. The Z factor is a function of gas gravity, pressure, temperature and the critical properties and it quantifies the real fluid volumetric behavior with respect to the behavior of an ideal fluid. There are a number of methods for estimating the Z factor of fluid systems. Some of the methods are

1. Sarem's method (1961)
2. Hall – Yarborough's method (1974)
3. Brill and Beggs' method (1974)
4. Dranchuk & Abou – Kassem's method (1975)
5. Gopal's method (1977)

All the above methods are aimed at generating Standing and Katz's Z factor chart by developing semi – empirical correlations. The Dranchuk & Abou – Kassem's method (1975) had shown the smallest absolute error among them. In this model, there are two methods for using the Z factor. One method directly uses the specified average Z factor and the other is computing the Z factor form the Standing – Katz chart by using the Dranchuk & Abou – Kassem correlation. The Dranchuk & Abou – Kassem correlation is shown in equation 4.38

$$Z = 1 + (A_1 + A_2/T_{pr} + A_3/T_{pr}^3 + A_4/T_{pr}^4 + A_5/T_{pr}^5)\rho_r + (A_6 + A_7/T_{pr} + A_8/T_{pr}^2)\rho_r^2 - A_9(A_7/T_{pr} + A_8/T_{pr}^2)\rho_r^5 + A_{10}(1 + A_{11}\rho_r^2)\rho_r^2/T_{pr}^3 \exp(-A_{11}\rho_r^2) \text{ ----- (4.38)}$$

where:

$\rho_r = 0.27P_{pr}/ZT_{pr}$ ----- (4.39)

$P_{pr} = P/P_c$ ------ (4.40)

$T_{pr} = T/T_c$ ----- (4.41)

ρ_r = Reduced density (dimensionless),

T_{pr} = Pseudo reduced temperature (dimensionless),

P_{pr} = Pseudo reduced pressure (dimensionless),

Z = Compressibility factor of the gas stream (dimensionless)

Table 4-1: Definitions of coefficients in the Dranchuk & Abou – Kassem Correlation

A_1	0.3265	A_7	- 0.7361
A_2	- 1.0700	A_8	0.1844
A_3	- 0.5339	A_9	0.1056
A_4	0.01569	A_{10}	0.6134
A_5	- 0.05165	A_{11}	0.7210
A_6	0.5475		

Gas Viscosity

As the gas stream flows through a pipe, some resistance will be offered by the pipe to the flow of gas. This is actually captured by the friction factor model under consideration and depending on the type of gas flow equation it is a function of Reynolds number which in turn is a function of the viscosity, density, diameter and velocity. The gas viscosity is often estimated by means of correlations or charts. In this model the Lee, Gonzalez and Eakin (1966) correlation is used for computing the gas viscosity. The correlation is shown in equation 4.42.

$$\mu_g = K * 10^{-4} \exp(X * \rho^y) \text{ ------ } (4.42)$$

where:

$$K = (9.4 + 0.02MWg)T^{1.5} / (209 + 19MWg + T) \text{ ------ } (4.43)$$

$$X = 3.5 + 989/T + 0.01MWg \text{ ------- } (4.44)$$

$$y = 2.4 - 0.2X \text{ ------- } (4.45)$$

μ_g = Viscosity of gas (cP),

T = Temperature (R),

MWg = Molecular weight of gas (lbm/lbmole)

4.7 Formulation of the Node Continuity Equations

Using the design equations for the pipe, compressor and the well, the node continuity equations are formulated. There are two fundamental methods to construct the node continuity equations. One is the P formulation approach and the other is the Q formulation approach. Both methods have the formulation of the node equations based on the principle of mass conservation, but in the Q formulation approach in addition to the node equations the loop equations are constructed which ensures energy conservation in the loop which is a direct consequence of Kirchoff's second law of network analysis. To demonstrate the difference between the two techniques consider the simple network shown in Figure 4-4.

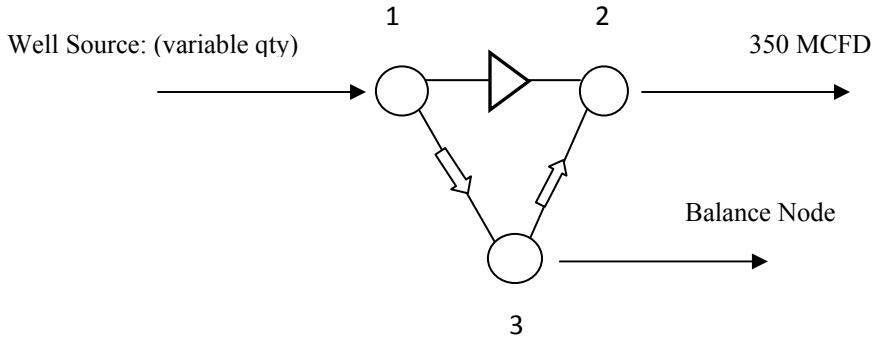

Figure 4-4: A simple network for illustrating development of node continuity equations

In Figure 4-4, the network has 3 nodes, 1 compressor and 2 pipes. Node 1 receives the supply from a well and node 2 and node 3 serve as the two demand points in the network. There is a compressor between nodes 1 and 2. At steady state conditions whatever flow comes into the network at node 1 leaves the network at nodes 2 and 3 respectively. The flow through the compressor pipe (connecting node 1 and node 2) can be taken as q_{COMP}, the flow in pipe 1 is q_1(connecting nodes 1 and 3) and the flow in pipe 2 is q_2 (connecting nodes 3 and 2).

4.7.1 The P Formulation Approach

If the node continuity equations are to be built based on the P formulation technique then the equations would look like as shown in equations 4.46, 4.47 and 4.48 where the primary unknowns are the nodal pressures. Equation 4.46 which shows the node continuity equation for node 1 where the flow coming into the network is from a well and the flow leaving node 1 are conveyed through compressor and pipe 1. Also the flow from a well, flow through a pipe and flow through the compressor are represented by their respective design equations as described in equations 4.34, 4.29 and 4.31 respectively in equation 4.46. Similar to equation 4.46 the node continuity equations are constructed for node 2 and node 3 which are shown in equations 4.47 and 4.48.

$$\text{Node 1: } C_{well}(P_{shut}^{\ 2} - P_1^{\ 2})^{n}_{well} - HP/(k_1(P_2/P_1)^{k}_3 - k_2) - C_{p1}(P_1 - P_3^{\ 2})^{1/n} = 0 \text{ ----- (4.46)}$$

$$\text{Node 2: } HP/(k_1(P_2/P_1)^{k}_3 - k_2) + C_{p2}(P_3^{\ 2} - P_2^{\ 2})^{1/n} - 350 = 0 \text{ ---- (4.47)}$$

$$\text{Node 3: } C_{p1}(P_1^{\ 2} - P_3^{\ 2})^{1/n} - C_{p2}(P_3^{\ 2} - P_2^{\ 2})^{1/n} - \text{balance} = 0 \text{ ----- (4.48)}$$

In a conventional surface gas network model, the first term in equation 4.46 would have been replaced by a constant supply specification. In this integrated model the constant supply flow rate node is treated as a well and to model the flow from a gas well, the gas well deliverability equation is used. If C_{well}, P_{shut} and n_{well} are known then equation 4.46 is still a function relating variables P_1 and P_2 just with a stronger dependency on P_1.

Though there are 3 nodes in the network and three node continuity equations can be constructed, at any node in the network a value of pressure must be explicitly specified which is a requirement to initiate the numerical solving technique described in section 4.9. The unknowns in equations 4.46 and 4.48 are the nodal pressure P_1 and P_3 if the pressure is specified at node 2. As we can see these are nonlinear equations that have to be solved simultaneously for the nodal pressures. Once the nodal pressures are known, the HP required for compression, deliverability from the

well and the flow rate in the respective pipes can be calculated. If there are N nodes there will be N-1 equations in the P formulation technique as one pressure value must be specified to solve the system of equations.

4.7.2 The Q Formulation Approach

In the Q formulation approach, the total number of node continuity equations required are "(N – 1) + L" equations. The L equations refer to the number of loop equations that can be formed by analyzing the number of loops present in the network. In Figure 4-4 there is one loop. The loop equation is shown in equation 4.52

$$\text{Node1: } 500 - q_1 - q_{COMP} = 0 \text{ ----- (4.49)}$$

$$\text{Node2: } q_{COMP} + q_2 - 350 = 0 \text{ ----- (4.50)}$$

$$\text{Node3: } q_1 - q_2 - \text{balance} = 0 \text{ ----- (4.51)}$$

$$\text{Loop1: } P_3^2(1 - \{1/k_1(k_2 + q_{COMP}HP)\}^{2/k}{}_3 - R_1 q_1^{\,n} - R_2 q_2^{\,n} = 0 \text{ ----- (4.52)}$$

As we can see from the node and the loop equations the primary unknown variables are the gas flows. The 'R' in equation 4.52 refers to the respective pipe resistivity which is the reciprocal of the pipe conductivity (C_p). Though there are 4 equations and 3 unknowns (q_1, q_2, q_{COMP}) one of the node equations is redundant and can be neglected to have finally 3 equations with 3 unknowns to solve for.

In this model the P approach methodology has been implemented as the total number of node continuity equations that has to be constructed would be (N-1) and there would be no requirement to build the loop equations.

4.8 The Concept of Balance Node

This model simulates the individual well production flow rates using the shut in pressure and the well performance constant which are unique to each producing well. Out of the nodes which are specified as demand points, one node acts as the balance node (without any demand specification). The net production of the balance node is the algebraic sum of the all the supply and demands in the network. The balance node creation is done in order to accommodate the production increase or decrease which can happen at the well heads when the network pressure changes so that steady state solution is always enforced. Without this balance node at steady state conditions the model will not be able to converge to a solution as the total output from the network now is a variable quantity. This balance node avoids the over specification of the problem. In the illustration network shown in Figure 4-4, node 2 or node 3 can be kept as the balance node. If node 2 is designated as the balance node then the demand at the node will not be exactly equal to 350 MCFD since the total input coming into the network at node 1 will be a variable quantity depending on the prevailing wellhead pressure at node 1 which in turn is dependent on the specified shut in pressure and well performance constant.

4.9 Numerical Solution

The node continuity equations are nonlinear in nature and have to be solved simultaneously. The methods that are generally used to solve non linear equations simultaneously are

1. Linear Theory Method
2. Generalized Newton Raphson Method
3. Hardy Cross Method

Out of the above three methods, the Newton Raphson iterative procedure is used in this model. Consider the following system of equations

$$F(x,y) = 0 \text{ ------ (4.53)}$$

$$G(x,y) = 0 \text{ ------ (4.54)}$$

We assume that (x_0,y_0) is an approximate solution. Suppose the true solution is $(x_0 + \Delta x_0)$ and $(y_0 + \Delta y_0)$ then each of these two values must satisfy equation 4.53 and 4.54 respectively. Now writing the Taylor series expansion for both the equations we get,

$$F(x_0 + \Delta x, y_0 + \Delta y) = F(x_0, y_0) + \Delta x \frac{\partial F}{\partial x}(x_{0,}y_{0)} + \Delta y \frac{\partial F}{\partial y}(x_{0,}y_{0)} + \ldots \text{ ----- (4.55)}$$

$$G(x_0 + \Delta x, y_0 + \Delta y) = G(x_0, y_0) + \Delta x \frac{\partial G}{\partial x}(x_{0,}y_{0)} + \Delta y \frac{\partial G}{\partial y}(x_{0,}y_{0)} + \cdots \text{ ----- (4.56)}$$

If we can approximate equations 4.55 and 4.56 such that,

$$F(x_0 + \Delta x, y_0 + \Delta y) \cong F(x_0, y_0) + \Delta x \frac{\partial F}{\partial x}(x_{0,}y_{0)} + \Delta y \frac{\partial F}{\partial y}(x_{0,}y_{0)} \cong 0 \text{ ----- (4.57)}$$

$$G(x_0 + \Delta x, y_0 + \Delta y) \cong G(x_0, y_0) + \Delta x \frac{\partial G}{\partial x}(x_{0,}y_{0)} + \Delta y \frac{\partial G}{\partial y}(x_{0,}y_{0)} \cong 0 \text{ ----- (4.58)}$$

Therefore,

$$\Delta x \frac{\partial F}{\partial x}(x_{0,}y_{0)} + \Delta y \frac{\partial F}{\partial y}(x_{0,}y_{0)} \cong -F(x_0, y_0) \text{ ----- (4.59)}$$

$$\Delta x \frac{\partial G}{\partial x}(x_{0,}y_{0)} + \Delta y \frac{\partial G}{\partial y}(x_{0,}y_{0)} \cong -G(x_0, y_0) \text{ ----- (4.60)}$$

Now there are two equations and two unknowns solving for $\Delta \boldsymbol{x}$, $\Delta \boldsymbol{y}$

$$\Delta y = G(x_0, y_0)\frac{\partial F}{\partial x}(x_{0,}y_{0)} - F(x_0, y_0)\frac{\partial G}{\partial x}(x_{0,}y_{0)} \Big/ \frac{\partial F}{\partial y}(x_{0,}y_{0)}\frac{\partial G}{\partial x}(x_{0,}y_{0)} - \frac{\partial G}{\partial y}(x_{0,}y_{0)}\frac{\partial F}{\partial x}(x_{0,}y_{0)} \text{-- (4.61)}$$

$$\Delta x = F(x_0, y_0)\frac{\partial G}{\partial y}(x_{0,}y_{0)} - G(x_0, y_0)\frac{\partial F}{\partial x}(x_{0,}y_{0)} \Big/ \frac{\partial F}{\partial y}(x_{0,}y_{0)}\frac{\partial G}{\partial x}(x_{0,}y_{0)} - \frac{\partial G}{\partial y}(x_{0,}y_{0)}\frac{\partial F}{\partial x}(x_{0,}y_{0)} \text{-- (4.62)}$$

The updated value of the approximate solution would be x_1, y_1

$$x_1 = x_0 + \Delta x \text{ ---- (4.63)}$$

$$y_1 = y_0 + \Delta y \text{ ---- (4.64)}$$

The iterative form of equations 4.74 and 4.75 would be

$$x_1^{(k+1)} = x_0^{(k)} - \{F(x_0, y_0)\frac{\partial F}{\partial x}(x_{0,}y_{0)} - G(x_0, y_0)\frac{\partial G}{\partial x}(x_{0,}y_{0)} \,/\, \frac{\partial F}{\partial y}(x_{0,}y_{0)}\frac{\partial G}{\partial x}(x_{0,}y_{0)} - \frac{\partial G}{\partial y}(x_{0,}y_{0)}\frac{\partial F}{\partial x}(x_{0,}y_{0)}\}^k \quad -(4.65)$$

$$y_1^{(k+1)} = y_0^{(k)} - \{G(x_0, y_0)\frac{\partial F}{\partial x}(x_{0,}y_{0)} - F(x_0, y_0)\frac{\partial G}{\partial x}(x_{0,}y_{0)} \,/\, \frac{\partial F}{\partial y}(x_{0,}y_{0)}\frac{\partial G}{\partial x}(x_{0,}y_{0)} - \frac{\partial G}{\partial y}(x_{0,}y_{0)}\frac{\partial F}{\partial x}(x_{0,}y_{0)}\}^k \text{ -- (4.66)}$$

where k is the iteration number and is = 0,1,2 …..

The procedure is repeated until $\Delta \boldsymbol{x}$, $\Delta \boldsymbol{y}$ in subsequent iterations approaches zero or is within a certain specified tolerance limit.

The equations if represented in the matrix would be of the form as shown in equation 4.67

$$\left(\begin{pmatrix} \frac{\partial F}{\partial x} & \frac{\partial F}{\partial y} \\ \frac{\partial G}{\partial x} & \frac{\partial G}{\partial y} \end{pmatrix}\right)^k \begin{pmatrix} \Delta x \\ \Delta y \end{pmatrix}^{k+1} = -\begin{pmatrix} F(x,y) \\ G(x,y) \end{pmatrix}^k \text{ ---- (4.67)}$$

The first matrix in the left hand side of equation 4.67 is called the Jacobian matrix, the second matrix is the delta matrix and the matrix in the right hand side is called the residual matrix. After every iteration the improved values of the variables x and y would be used to check such that the value of the residual matrix becomes smaller when compared to the previous iteration and finally approaches zero.

Every row of the Jacobian matrix essentially contains the node continuity equation with respect to that node and the total number of rows is equal to the number of nodes in the network but the total number of node continuity equations required is (N-1). This is because the Newton Raphson method needs at least one value of pressure to be specified at any node in the network.

With the initial assumption of a single value of pressure at any node in the network the Newton Raphson iterative procedure is started and it is executed till the difference in the value of pressure in the current iteration and the previous iteration at all the nodes in the delta matrix is within a tolerance level which in turn makes the residual matrix approach zero.

In this model to increase the rate of convergence of the iteration process, all the nodes at which the node pressures has to be calculated is assigned a value of pressure corresponding to the value of well head pressure recorded at that node from the production data. This significantly reduces the total number of iterations as the final value of pressures calculated at the different nodes in the network will not be far away from the initial assigned value. Also one other additional feature that has been included in this model for increasing the rate of convergence is the Stoner's acceleration method. In this method the value of the pressure at any node is improved after every third iteration based on the improvement ratio which is defined as ratio of the change in pressure value in the (k + 3) iteration to the change in value of pressure in the k^{th} iteration. Based on the improvement ratio different acceleration parameters are employed and the updated value of the pressure in the k^{th} iteration would be old value of pressure in the previous iteration plus the change in pressure value multiplied by the acceleration parameter.

4.10 Stages of Model Execution

The model has been built to execute in stages. The very first step is the data acquisition stage where the input information with regard to the facilities, node and the fluid are provided in a specific format as shown in Figure. 4-6 are read by the model. This is done in order to verify that the given information is consistent with respect to the given input conditions. The model initially checks that the given network information satisfies one of the following mathematical constraints as shown in equation 4.68 or 4.69 depending on the existence of pipe loops in the pipe network.

Number of loops = Number of pipes + Number of compressors – (Number of nodes -1) ---- (4.68)

Number of nodes = Number of pipes + Number of compressors + 1 ---- (4.69)

Equation 4.68 is valid for networks with loops and equation 4.69 is valid for loop less networks.

If any one of the above conditions is not satisfied then the model stops the execution and prompts the user to correct the input information. Once the above condition is satisfied the model starts analyzing the facilities information to check for their location in the network system. It checks that a pipe is defined completely starting with the location of the pipe in the network by analyzing the upstream node, downstream node and the physical properties. If any of the information is missing or inconsistent then a message is prompted to the user to correct the input file. The compressors in the network are defined in the same way as the pipe but only the upstream and the downstream node information is given the rest of the properties are described by the number zero. This is the method used to identify compressors present in the network. Next, the node along with the pressure specification value is read by the model. Then the model starts to read the compressor description information such as the compressor constants, choice of HP or pressure specification and the fuel factor information. At this point the model has read and stored all information related to the node connecting elements. Now the model proceeds to read the information related to the nodes in the system. The model identifies whether the correct node information is given with respect to node type described and that all the nodes in the system are defined. Once this is done the model reads the gas loss factor information if specified. Additionally, the model reads the base conditions of pressure and temperature, type of flow equation that has to be used by the model to calculate the nodal pressures, type of Jacobian matrix construction and the information related to pressure initialization.

The communication between supply nodes and the demand nodes conveyed by the facilities present in the network is a vital factor to ensure that the pipe network under consideration is complete and can be modeled as a single interconnected system. To ensure the connectivity of the network and based on the information acquired by the model related to the nodes and node connecting elements,

the model carries out the network interconnectivity test. In the interconnectivity test, the model starts sweeping the system starting from the node where the pressure specification was done to ensure that

1. all the nodes in the system are encountered while sweeping to check the establishment of full network communication
2. all pipes in the system has at least one incoming and outgoing flow for steady state solution
3. at least two pipes are connected to a node except in the case of a supply or a demand node and to identify the presence of any dead end node.

If the network is fully communicating after the interconnectivity test, the model proceeds to the final stage where the Jacobian matrix is built to solve the node continuity equations.

4.11 Sample Demonstration Network

Consider the network shown in Figure 4-5. The network has 5 pipes, 5 nodes, 2 loops and 1 compressor. The compressor is located between nodes 1 and 4. There are 3 producing wells supplying gas at nodes 1, 2 and 3 respectively. There are two loops. Loop1 bounded by nodes 1, 2, 3 and 4 and loop 2 bounded by nodes 4, 3 and 5. The compressor constants k_1, k_2 and k_3 are 0.194, 0.194 and 0.230 respectively. The network is a horizontal system with no elevation. The gas flowing in the network is assumed to be mostly methane with a specific gravity of 0.58. Since the temperature is assumed to be constant, an average flowing temperature of 60F is taken for the gas. The flow efficiencies of all the pipes are assumed to be 1 with roughness 0.001”. The input file to the model looks like as shown in Figure 4-6.

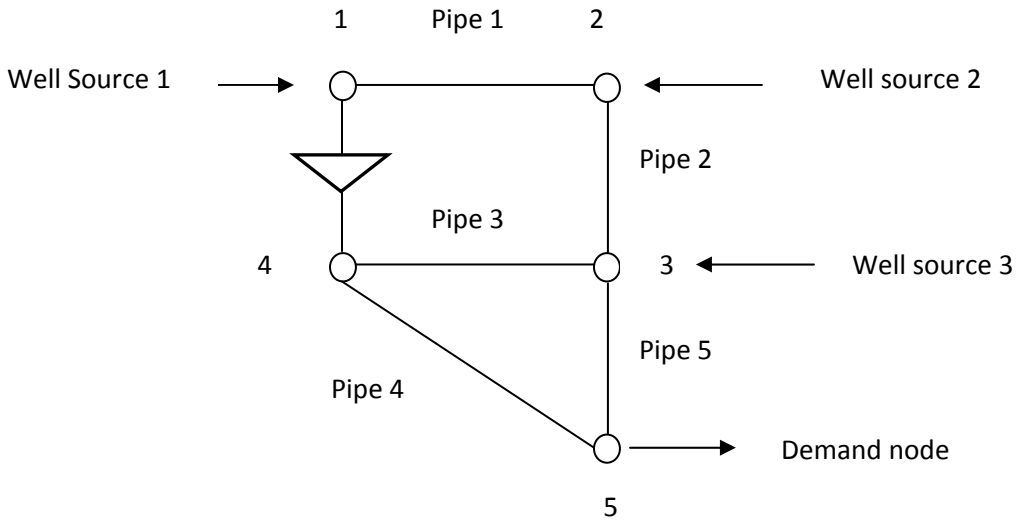

Figure 4-5: Network for model functioning demonstration

As we can see from Figure 4-6, the number of pipes denoted as 'NPIPES' is 5. Similarly the information about number of nodes, loops and compressors are also provided. The pipe properties of all the pipes such as the upstream, downstream nodes, length, inner diameter, roughness, number of slopes (if the pipe has more than one length section), and elevations corresponding to number of slopes are provided as a detailed description. Compressor location in the network is similar to a pipe but all other properties such as length, inner diameter etc are entered as zero. This is a method used for identification of compressors present in the network. The Newton Raphson procedure requires a value of pressure to be specified which is provided as input with the node and the corresponding pressure specification. Compressor description is provided by specifying the performance constants k_1, k_2, k_3 and the suction or discharge pressure or HP specification with the additional option to specify the fuel factor information. The information related to the nodes in the network depends on the type of node. In this model, there can be three possible types of nodes.They are the inter node/demand node, well node and the balance node. With respect to this illustration network, out of the 5 nodes, 3 are well nodes, 1 inter node and a balance node. The well nodes indicated by '2' have to be specified with C_{well}, P_{shut} and n_{well}. The inter node/demand node indicated by '1' have to specified with the respective flow rates and the

balance node indicated by ‘0’ needs no specification. The ‘Gas Loss Factor’ when specified accounts for the well head losses in the network. The fluid properties such as specific gravity, Z factor are specified though the model has the option to calculate the Z factor. The pipe flow equation that has to be used to model the network has to be specified. The model converges faster if the numerical type Jacobian matrix is used which is basically built on the principle backward finite difference method. The pressure initialization might not be significant for a simple network like this but as the network becomes more complex, this initialization is necessary to keep the iterated values in the neighborhood of the final solution and to increase the convergence rate.

```
TITLE:-SAMPLE_DEMONSTRATION_FILE_2009
NPIPES
5
NNODES
5
NLOOPS ( NLOOPS = NPIPES + NCOMPR - NNODES + 1 )
2
NCOMPR
1
PIPE(I)/JUP(I)/JDN(I)/fe  /Tav(F)/ID(in)/e(in)/#slopes  /L's-ft(#slopes)    /   ActualElevations-ft(#slopes+1)fromUPtoDOWN
    1   1       4    0     0      0      0          0          0                  0d0 0d0
    2   1       2    1.00  60d0   3.0    0.001d0    1          10000              0d0 0d0
    3   2       3    1.00  60d0   4.0    0.001d0    1          6000               0d0 0d0
    4   3       4    1.00  60d0   3.0    0.001d0    1          10000              0d0 0d0
    5   4       5    1.00  60d0   5.0    0.001d0    1          5000               0d0 0d0
    6   3       5    1.00  60d0   6.0    0.001d0    1          10000              0d0 0d0
NODE-WITH-PRESSURE-SPECIFICATION: NodeNumber/Pressure(psia)
5    150.0d0
COMPRESSOR INFO:  COMP.No. / k1    / k2 /    k3  / CHOICE /Specf-Value/ FuelRatio(SCF/hr/HP) [CHOICE:1=HP Sp;2=Pd Sp;3=Ps Sp]
                     1      0.194   0.23   0.194    3      110            0
NODE#/NODETYPE[0,1,or 2] [0=BALANCE Node;1=ConstQ;2=IPR]/ NODEINFO [Type1=Qconst; Type2=C(MSCFD/psi^2n),Pshut(psia),n ]
1   2   1.760   350d0   0.75d0
2   2   0.847   250d0   0.75d0
3   2   3.030   200d0   0.75d0
4   1   0d0
5   0   -15000.0d0
GAS LOSS FACTOR [ Fraction -- from 0.0 (default) to 0.5 ] -- "Fraction of wellhead gas unaccounted for at sales"
0.0d0
Fluid information: Gas Gravity / Zav (Enter Zav = 0.00 if you want Z's from Standing Katz)
0.58   0.90
Base Conditions: Psc (psia) / Tsc (F)
14.7   60.0
Type of Flow Equation to be Used (1=Generalized with rig. friction factor; 2= Weymouth; 3=Panh-A; 4=Panh-B)
2
Type of Jacobian Entry Calculation (1=Numerical ; 2=Analytical)
1
PressInitial.txt file (0=Not needed;1=Create it;2=Use it when available for P-initialization;3=Use it for P-initialization and overwrite existing file)
0
```

Figure 4-6: Input file to the model

Once all the inputs are provided, the model is executed and it begins by analyzing the network for any inconsistencies in the specified input and proceeds to solve the node continuity equations if the network is communicating effectively from the first node to the last node. During the iteration process the model displays the iteration number, maximum value in the delta matrix, maximum

value in the residual matrix and the row number associated with these maximums. The output of the model after achieving convergence would look like as shown in Figure 4-7. The total network deliverability is predicted to be 16342 .77 MCFD for the specified network operating conditions. This total deliverability is a function of well head pressures and the deliverability information of the wells in the network. If there is more backpressure at the well heads due to a change in the network pressure as a result of new well tie – ins, the deliverability may decrease.

```
TITLE:-SAMPLE_DEMONSTRATION_FILE_2009



P,C,Q PREDICTIONS BASED ON Weymouth EQUATION:
P(   1)=     110.00 psia - C(   1)= ********** - Q(   1)=    12247.645 MSCFD
P(   2)=     167.22 psia - C(   2)=      12.610 - Q(   2)=    -1588.080 MSCFD
P(   3)=     166.46 psia - C(   3)=      35.059 - Q(   3)=      557.857 MSCFD
P(   4)=     213.35 psia - C(   4)=      12.610 - Q(   4)=    -1682.876 MSCFD
P(   5)=     150.00 psia - C(   5)=      69.634 - Q(   5)=    10564.769 MSCFD
P(****)= ********** psia - C(   6)=      80.067 - Q(   6)=     5778.001 MSCFD
COMPRESSOR (          1 ) Horsepower =    391.062458539670       HP

TITLE:-SAMPLE_DEMONSTRATION_FILE_2009



PRODUCTION FROM VARIABLE-FLOW NODES [Balance Node and Nodes Type 2, if any]
NODE=   1 - Cwell=   1.76; Pshut=   350.00; n= 0.75 - Qwell=  10659.565 MSCFD
NODE=   2 - Cwell=   0.85; Pshut=   250.00; n= 0.75 - Qwell=   2145.937 MSCFD
NODE=   3 - Cwell=   3.03; Pshut=   200.00; n= 0.75 - Qwell=   3537.268 MSCFD
NODE=   5 - ** BALANCE NODE **                      - Qbalc= -16342.770 MSCFD
```

Figure 4-7: Output of the model

Chapter 5

CASE STUDIES

5.1 Natural Gas Gathering and Production System – Network Information

The gas gathering and production system for which the model was developed is located near the town of Snow Shoe, Pennsylvania. The gathering system of interest handles production from about 600 shallow gas wells ranging in depth from 3500’ to 4500’ and consists of few hundred miles of gathering lines of various sizes. Figure 5-1 shows the location of the network in Snow Shoe indicated by the number 1. The letter A indicates the location of the Pennsylvania State University with respect to Snow Shoe. The network is present in the Center and Clinton counties of the interstate highway 80 west.

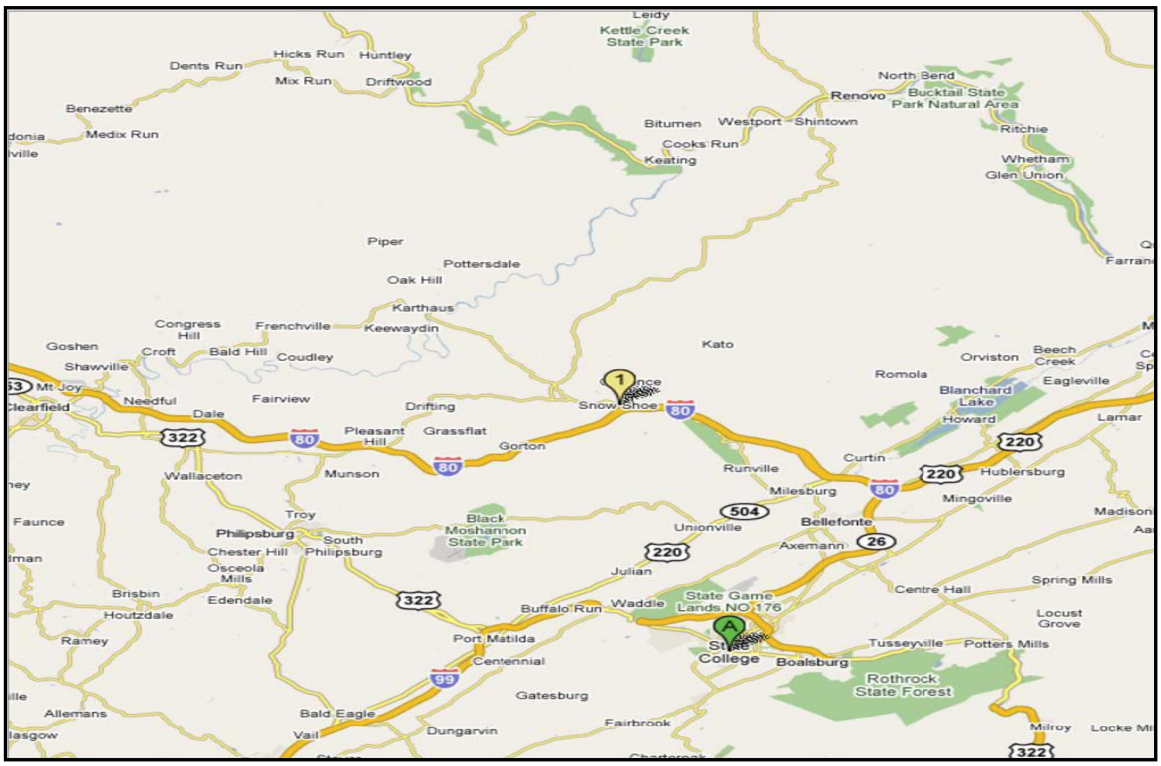

Figure 5-1: Aerial location of the network under study (Source: Google maps)

The topographical map of the network is shown in Figure 5-2. In Figure 5 – 2, the entire pipeline network has been classified as the North, Middle and South sections respectively for ease of analysis. There are 5 compressor stations and 4 sales points as shown in Figure 5-2. Flow through the system is powered by several compressors located at the five different locations in the system. The four different sales points are located close to the distributing or the main trunk line where custody transfer takes place. Though this field is a collection of hundreds of mature stripper wells, it still has the potential to harvest new volumes of natural gas from projected drilling activity. The production rates of the wells range between a thousand cubic feet to two hundred and fifty thousand cubic feet.

The GPM (gallons per million) analysis of the gas shows that GPM < 1, which is typical of a very lean gas that comes from a non-associated gas reservoir. The amount of heavy components in the gas mixture is so small that hydrocarbon condensation has been ruled as highly unlikely in this network. Based on the study of the available chromatographic analysis of gases at the custody transfer points, a representative gas gravity of 0.58 is used in the analysis. Over the past one year approximately 20 – 30 new wells were added to the system. The entire network system spans across an area of 600 square miles. Based on the gas gravity and the pseudo critical properties, the Z factor of the produced gas is expected to remain between 0.9 – 1. Thus an average Z factor of 0.95 is used in the study. The network runs over a hilly terrain with the highest elevation being 2100 feet and the lowest elevation being 500 ft above sea level. The pipes connected in system comprise both plastic and steel pipes. The maximum and minimum diameters of the pipes in the system are 6 inch and 1.5 inch respectively. The colors orange, red, green, blue and pink indicate pipe diameters 1.58”, 2”, 2.38”, 4”, 6” respectively. The daily average output from the entire network is around 5 million cubic feet of gas. The north section produces about 1500 MCFD of gas and has one sales point with a peak demand of 500 MCFD of gas. The middle section

produces around 2100 MCFD of gas and has one sales point with a demand of 4000 MCFD and the south section produces about 1500 MCFD of gas and has two sales points with a total demand of 700 MCFD.

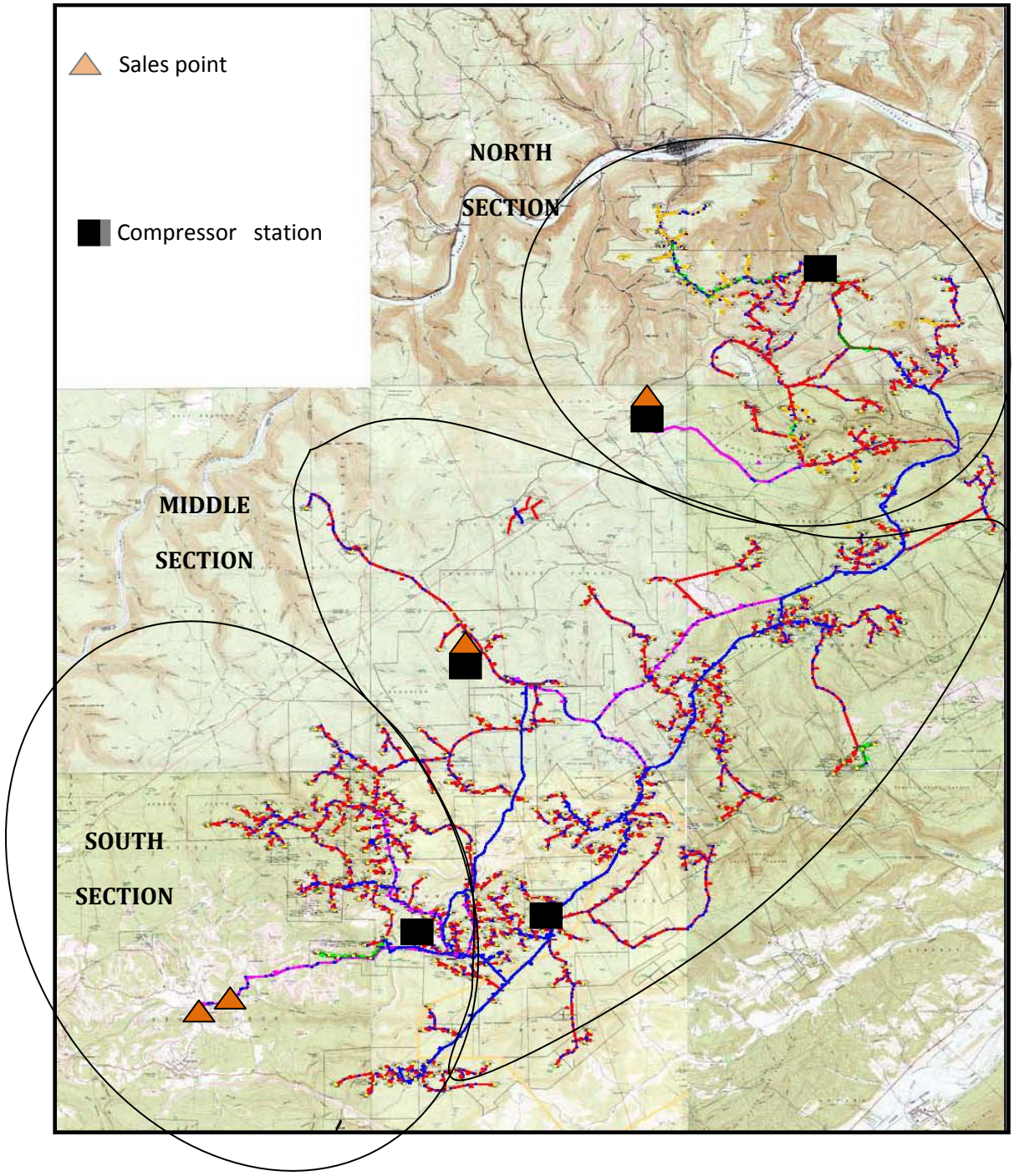

Figure 5-2: Topographical map of the network under study

5.2 Estimation of Well Shut in Pressure and Well Performance Constant

One of the first objectives of this study was to quantify the influence of changes in surface network conditions on the deliverability of the wells. Therefore Inflow Performance Relationship (IPR) parameters needed to be known for all existing wells in the system. A common correlation used in the field of gas well testing to characterize the deliverability from a producing well (Kelkar, 2008) as described in section 4.2 is shown below.

$$\mathbf{q_{sc} = Cwell\left(Pshut^2 - Pwh^2\right)^{nwell}} \quad \text{------} \quad \mathbf{(5.1)}$$

where,

q_{sc} = Gas production flowrate (MCFD)

C_{well} = Well performance constant, a function of rock and fluid properties, formation thickness, external boundary radius and wellbore radius (MCFD/psi^{2nwell})

P_{shut} = Well head shut in pressure at the average reservoir pressure (psia)

P_{wh} = Flowing well head pressure (psia)

n_{well} = Value to characterize turbulent or laminar flow of fluid and varies between 0.5 and 1.0 with 0.5 representing completely turbulent flow and 1 representing completely laminar flow

Equation 5.1 was first proposed in 1936 on a study using backpressure data to assess the deliverability of gas wells by Rawlins and Schellardt. The significance of the above equation is that once we are able to characterize the values of C_{well}(well performance constant) , P_{shut} (shut in pressure) and n_{well} for a particular well, we can calculate the flow rate produced by the well for different well head pressures for that particular well. Gas well IPR's are typically calculated by performing deliverability well test on the well. However, this data was not readily available and the operators expressed significant concerns about undertaking a well test campaign for 500 or more active producing wells, considering the tight nature of the reservoir. The data we have in hand are the well head pressures and corresponding flow rates associated with the wells. Using

the above equation, a plot between P_{wh}^2 and $q_{sc}^{(1/nwell)}$ should yield a straight line with a negative slope equal to $(1/C_{well})^{(1/nwell)}$ and intercept equal to P_{shut}^2 as shown in Figure 5-3. From the value of the slope and intercept we can get the value of C_{well} and P_{shut} for that particular well. Since n_{well} is not known beforehand, a best fit match analysis is required for several different values of n_{well} ranging from 0.5 to 1.0.

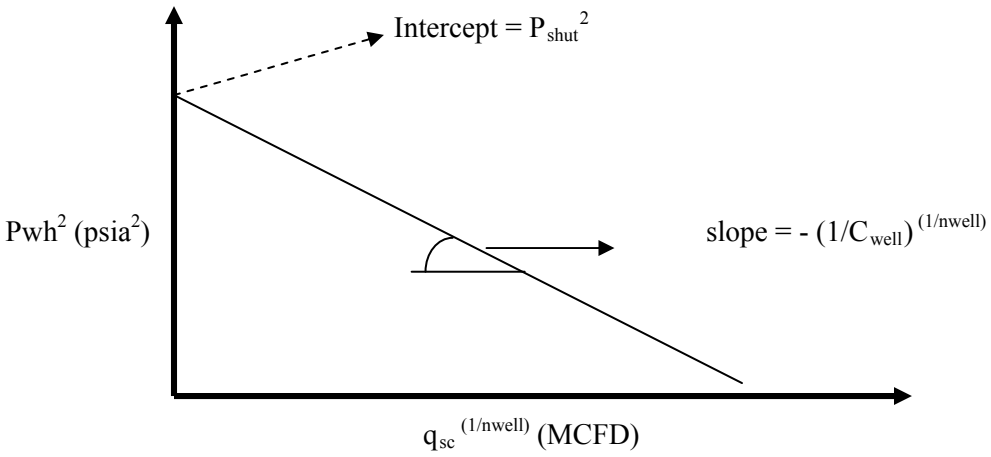

Figure 5-3: A well deliverability plot

5.3 IPR Estimation

An arbitrary selection of producing wells in the Northern section of the Snow Shoe network was done to identify the relationship between well head pressure and flow rate of the well. Using the well head pressure (P_{wh}) and flow rate (q_{sc}) data for these wells a plot of P_{wh} vs q_{sc} was constructed to identify the trend in the plots. To get a straight line in the Pwh^2 vs $q_{sc}^{(1/nwell)}$ plot as shown in Figure 5-3, one should obtain a negative slope behavior in P_{wh} vs q_{sc} plot , that is higher the flow rate the lesser associated wellhead pressure. 70% of the screened wells showed more or less the expected trend while the remaining did not have any identifiable relationship. Examples of wells showing the expected behavior is shown in Figures 5-4 (well: 678#02) and

5-5(well:678#04). Some wells did not have any relationship between the well head pressure and the flow rate of the well as shown in Figures 5-6(well: 678#52) and 5-7(well:678#14).

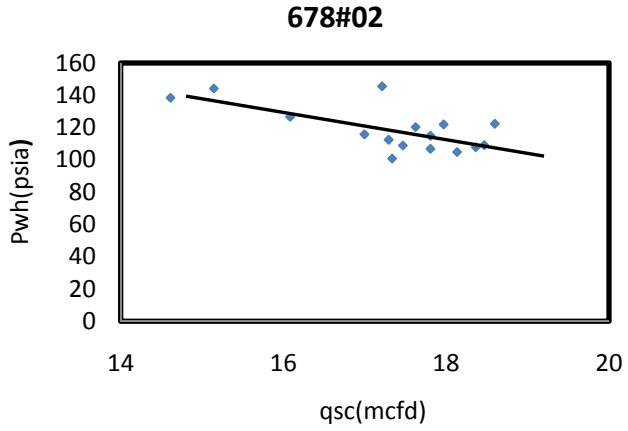

Figure 5-4: P_{wh} vs. q_{sc} (well:678 #02) – Expected trend

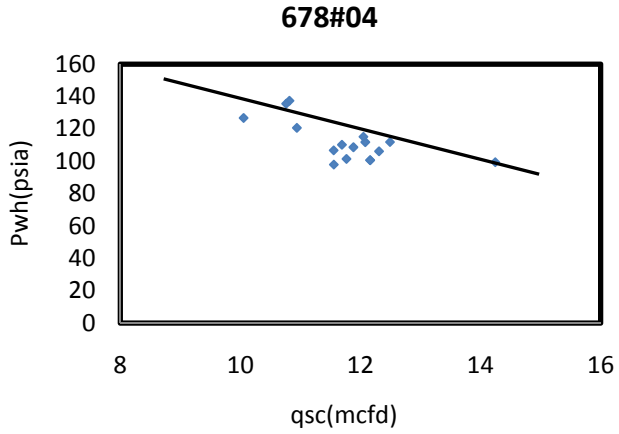

Figure 5-5: P_{wh} vs. q_{sc} (well: 678 #04) – Expected trend

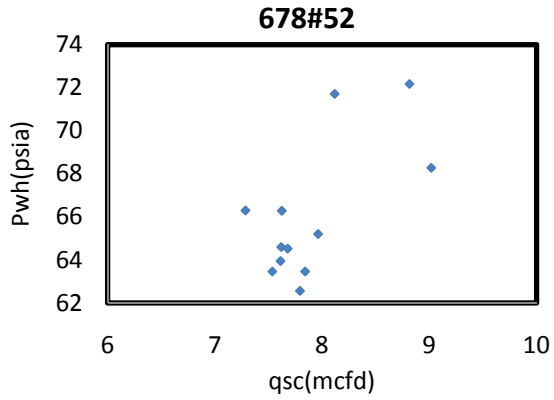

Figure 5-6: P_{wh} vs. q_{sc} (well:678 #52) – Unidentifiable trend

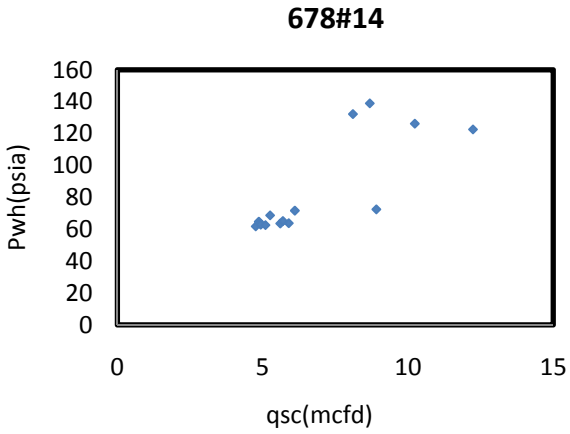

Figure 5-7: P_{wh} vs. q_{sc} (well: 678 #14) – Unidentifiable trend

The plot (Pwh^2 and $q_{sc}^{(1/nwell)}$) shown in Figure 5-3 was constructed for wells which had the expected relationship between flow rate and pressure. This plot was used to calculate the C_{well} (well performance constant) and P_{shut} (shut in pressure) for a well. Due to the uncertainty about the appropriate n_{well} – value, the plots were constructed for a 'n_{well}' value of 0.5, 0.6, 0.7, 0.8, 0.9 and 1 to study the variation in the calculated values of P_{shut} and C_{well}. If the trend of the straight line in the plot was similar to the trend represented in Figure 5 -3 and the R^2 value of the fit was close to 1 then the P_{shut} and the C_{well} were calculated from the intercept and slope of the straight line. If the straight line had the necessary trend but the R^2 value of the fit was very less, then the plot was reconstructed again for such wells with some of the data points removed so as to

increase the R^2 value of the fit and then P_{shut} and C_{well} were calculated. The wells which did not show the expected deliverability behavior, the P_{shut} was calculated first by approximating the straight line fit as a horizontal line parallel to the horizontal axis passing through most of the data points and reading the P_{shut} from the intercept. Then the C_{well} was calculated by using equation 5.1 and the production data for that well. Examples of plots for well 678#01@ n_{well} =0.9 and for well 678#04@ n_{well} =0.5 are shown in Figure 5-8 and Figure 5-9 respectively. The values of C_{well} and P_{shut} calculated for the above two wells are shown in the Tables 5.1 & 5.2 respectively.

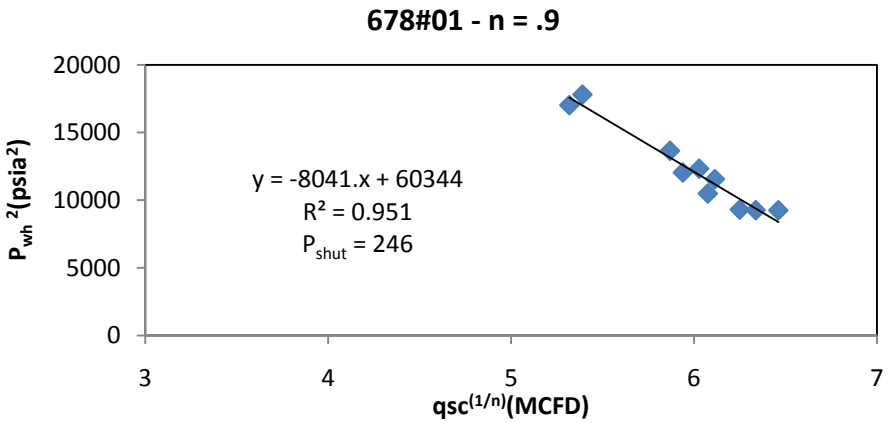

Figure 5-8: Pwh^2 vs $q_{sc}^{(1/nwell)}$ for well 678#01@ n_{well} = 0.9

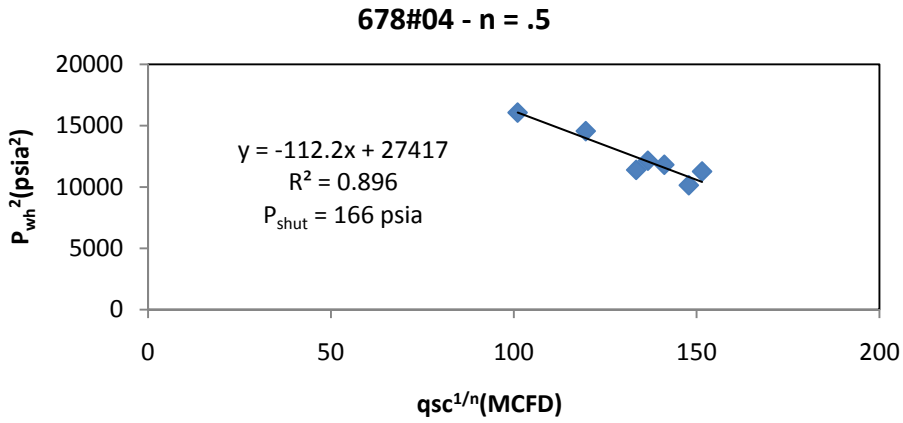

Figure 5-9: Pwh^2 vs $q_{sc}^{(1/nwell)}$ for well 678#04@ n_{well} = 0.5

Table 5.1: Deliverability parameter information for well#678-02

678#01				
n_{well}	**P_{shut} (psia)**	**m(slope)**	**C (MCFD/psi^{2nwell})**	**R^2**
0.5	199	-1084	0.03037	0.948
0.6	212	-2214	0.00984	0.949
0.7	224	-3774	0.00314	0.950
0.8	235	-5731	0.00098	0.950
0.9	246	-8041	0.00031	0.951
1	256	-10663	0.00009	0.951

Table 5.2: Deliverability parameter information for well# 678-04

678#04				
n_{well}	**Pshut (psia)**	**m (slope)**	**C (MCFD/psi^{2nwell})**	**R^2**
0.5	166	-112.2	0.09441	0.896
0.6	174	-301.5	0.03254	0.897
0.7	182	-625.3	0.01103	0.898
0.8	190	-1100	0.00369	0.899
0.9	197	-1730	0.00122	0.889
1	204	-2514	0.0004	0.879

From Tables 5.1 & 5.2, the values of shut in pressure (P_{shut}) calculated for the various values of n_{well}, increases as the value of n_{well} increases from 0.5 to 1.0. Also we can see that the R^2 value for the different values of 'n_{well}' does not improve significantly for any value of n_{well} as they hover around the same value which indicates the range of n_{well} is very small to create any improvement in the best straight line fit. With this preliminary analysis it was decided to use a n_{well} of 0.75 for further study uniformly for all the producing wells. The C_{well} and P_{shut} for all the wells in the

north section of the network was calculated from the P_{wh}^2 and $q_{sc}^{(1/n)}$ plot. Figure 5 -10 and 5 -11 shows the P_{shut}'s and C_{well}'s for all the wells in this section.

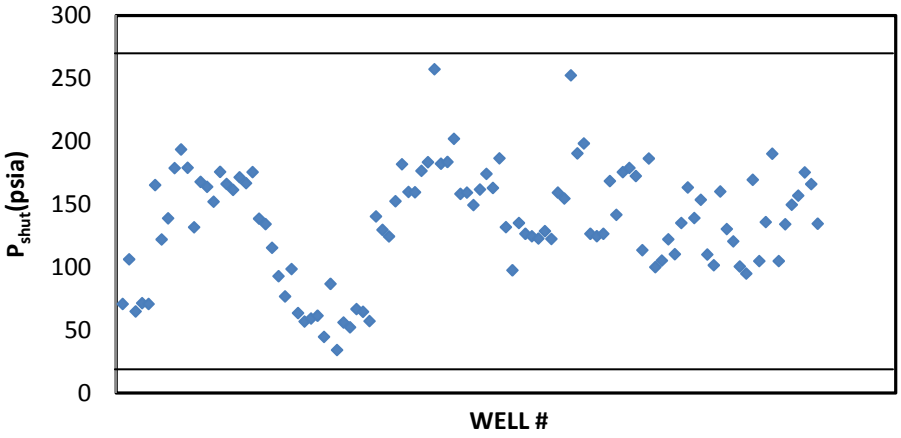

Figure 5-10: Shut in pressure for wells in the north section of the network

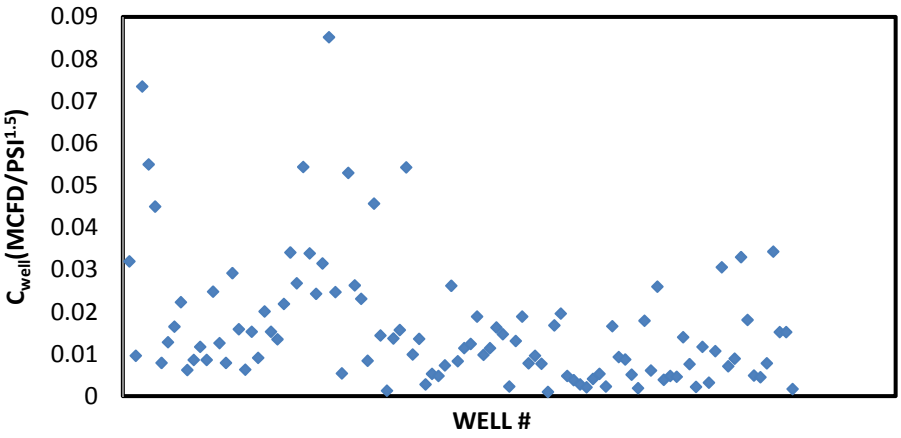

Figure 5-11: Well performance constant for wells in the north section of the network

In Figure 5 -10, we can see that the shut in pressures of the wells in this section fall between the range of 30 psia and 260 psia .The operators indicated that these shut in pressure calculated from the P_{wh}^2 and $q_{sc}^{(1/n)}$ plot shown in Figure 5-10, were on the lower side. Therefore they provided an updated value for the shut in pressures for the wells in the network. By using these new shut in pressures the C_{well}'s for the wells in this section was recalculated using the

production history of the wells and equation 5.1. Figure 5- 12 and 5 -13 shows the revised value of shut in pressures and well performance constants respectively.

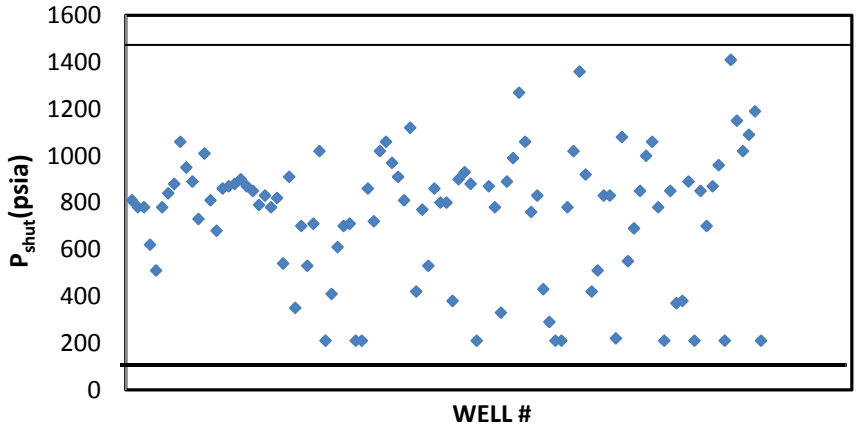

Figure 5 -12: Revised shut in pressures for wells in the north section

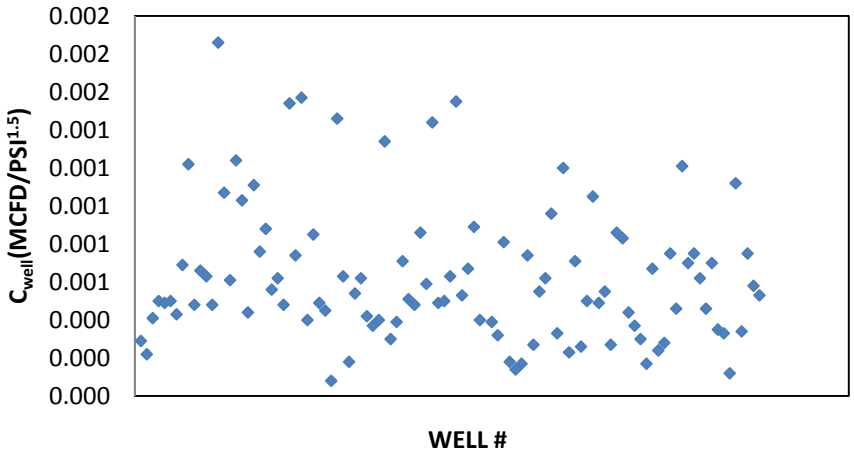

Figure 5 -13: Revised well performance constants for wells in the north section

When compared to the shut in pressures shown in Figure 5 -10, the new shut in pressures are on the higher side (range between 200 psia and 1500 psia). As a result of this, the calculated $C_{well's}$ shown in Figure 5 -13 have become considerably lower in comparison with $C_{well's}$ in Figure 5 -11. Even though Figure 5- 12 shows a 4 –fold increase in $P_{shut's}$, operators indicated that the study should be based on them.

5.4 Initial IPR Modeling and Results

To study the deliverability predictions of the model, an initial IPR study was undertaken by modeling a section within the north section of the system by using the well performance constant and shut in pressure calculated from the P_{wh}^2 and $q_{sc}^{(1/n)}$ plot. Figure 5-14 shows the area of the network (identified by the blue boundary) under consideration. The Pwh^2 and $q_{sc}^{(1/n)}$ deliverability plots were constructed for all the producing wells in the network and the shut in pressure and the well performance constants were calculated as explained in section 5.3. The deliverability plots for some the wells in this section are represented in Figures 5-15.

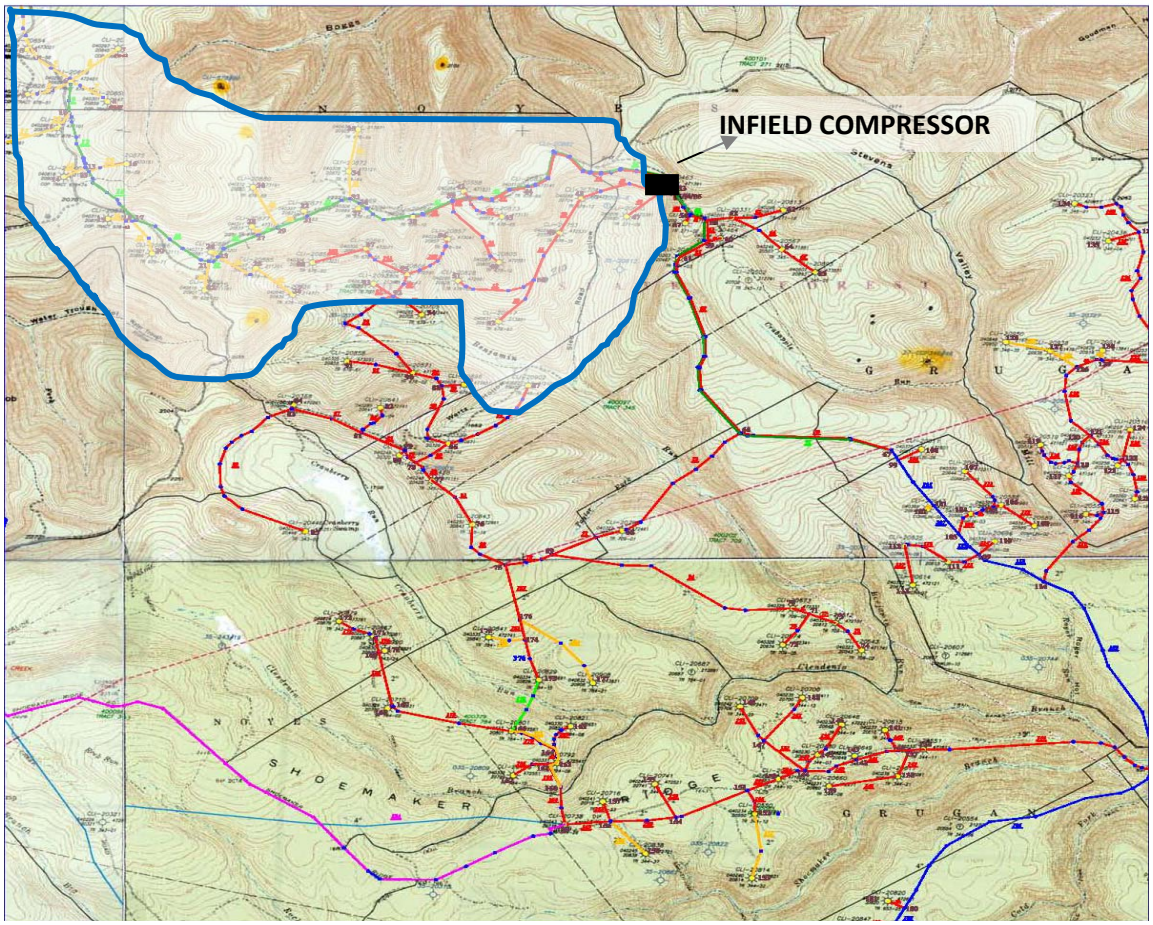

Figure 5-14: Topographical map showing the area of the North section considered for the initial study

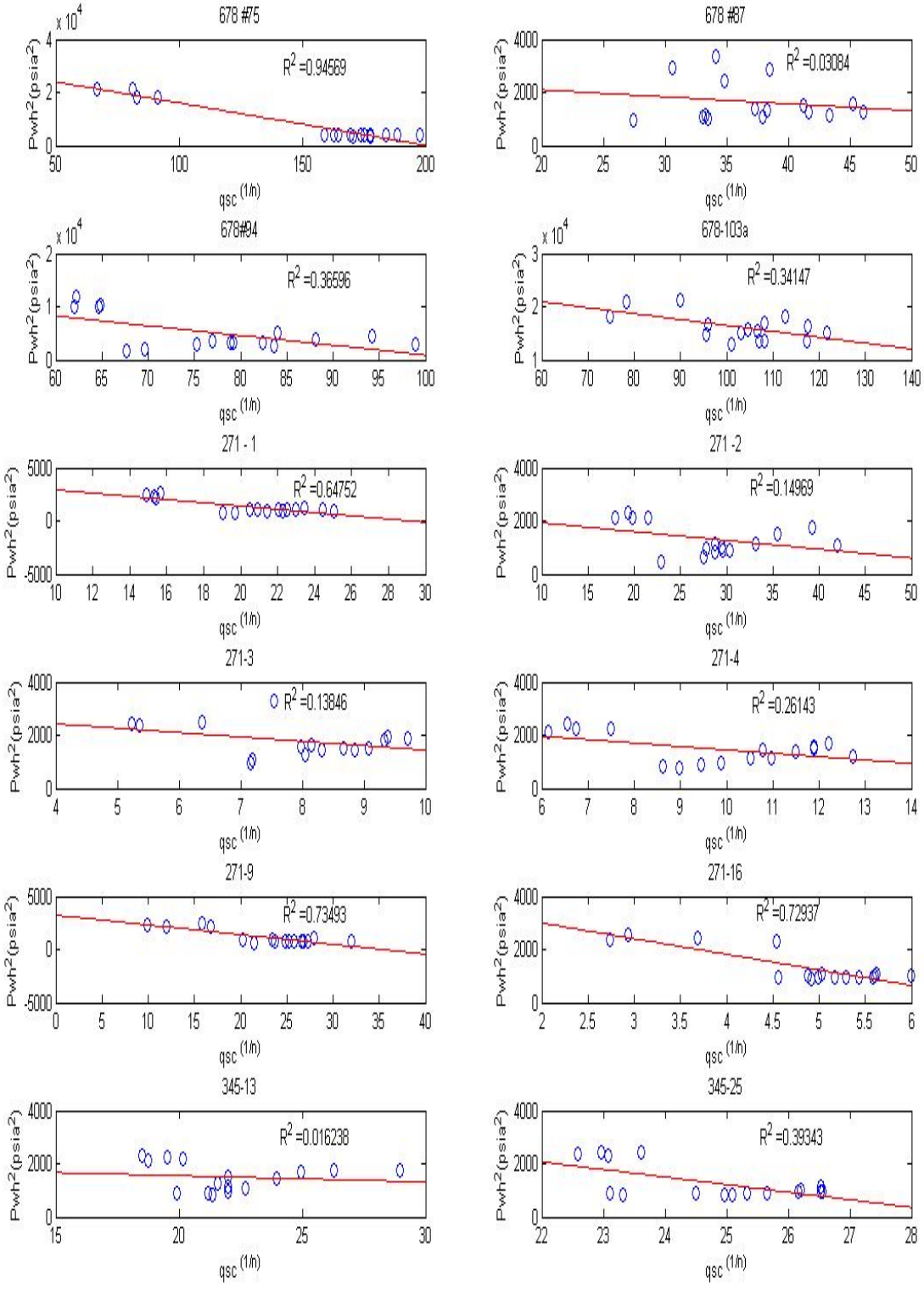

Figure 5-15: Deliverability plots for some wells in the north section of the network

The C_{well} and P_{shut} for all the wells shown in the above plots were calculated from the slope and the intercept of the respective deliverability plots. The area under consideration is truncated at the infield compressor suction point as shown in Figure 5-14. With the pressure specification at the suction node, the initial modeling was carried out to see the deliverability predictions. Previous work done to characterize the performance of this network found that the best predictions were obtained when Panhandle –B pipe flow equation was used (Krishnamurthy, 2008). Therefore the pipe flow equation which was used for the modeling process was Panhandle – B. The cross plot of model predicted flow rates and the field flow rate is shown in Figure 5-16. As we can see the model predictions are good. The cross plots for 11 months of production data was generated and the best match is shown in Figure 5-16.

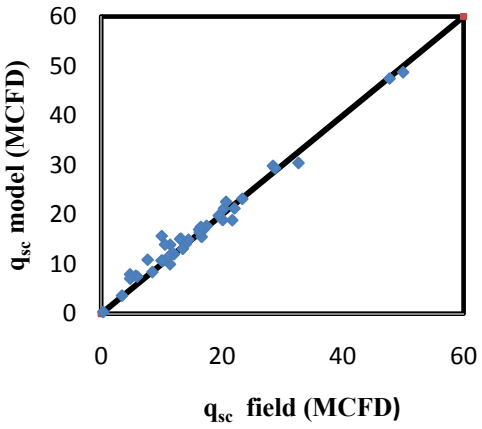

Figure 5-16: Cross plot comparing model predicted flow rates and field flow rates for initial study

The next step in the modeling process was to see how the predictions varied after the inclusion of new wells which were added to the same area of interest in the north section of the network. The cross plot for this analysis is shown in Figure 5-17. In Figure 5-17, we can see that we are able to get a good match with the field data. In addition to the predictions, we can observe that for some wells the production became nil. This occurrence is a direct consequence of the

change in well head pressure of those wells due to the inclusion of new wells to the network. As the prevailing well head pressure became more than the shut in pressure of the well it naturally shut down.

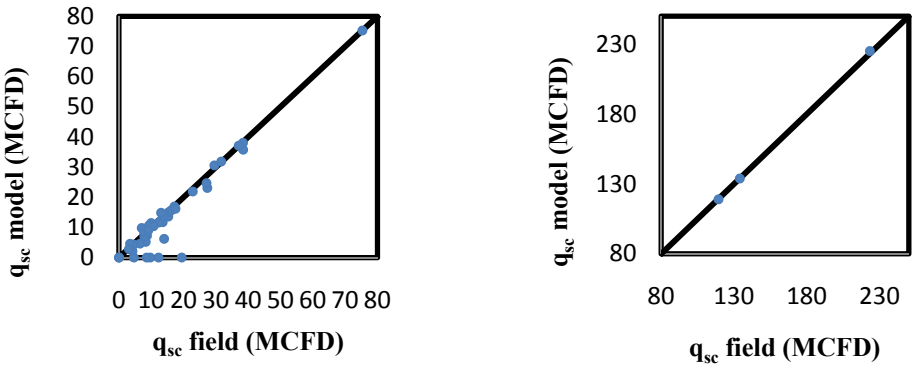

Figure 5-17: Cross plots showing predictions with new wells included: Flow from 0 to 80MSCFD (Left Plot) and from 80 to 250 MSCFD (Right Plot)

Table 5-3 shows the comparison between model and field predicted flow rates for the wells shown in the cross plot in Figure 5-17. The rows in Table 5-3 that are highlighted in yellow show the wells which continued to produce in the field after the new volume inclusion though the model predicts them to be shut. The rows highlighted in blue indicate the wells that actually ceased to produce and the model also show them to be shut. The rows highlighted in pink show the new wells which came online into the system. The wells which were predicted by the model to be shut but continued to produce in the field had no proper deliverability fit and the shut in pressure and well performance constant had to be approximated. This could be one of the reasons why the model predicts them to produce. The next step in the modeling process was to see the model predictions for the entire north section of the network. The shut in pressure and the well performance constant of the remaining wells were generated and the entire north section was modeled. Figure 5-18a and 5-18b show the cross plots comparing the model and field predictions.

Table 5-3: Comparison of model and field predicted flow rates

Well name	q_{sc} model(MCFD)	q_{sc} field(MCFD)
678 #14	0	12.24
678 #16	0	4.62
678 #58	0	9.68
678 #66	0	19.43
678 #50	0	8.58
678 #57	9.84	7.07
678 #51	2.18	4.19
678 #53	9.18	9.05
678 #75	30.56	29.55
678 #74	11.89	12.59
678 #59	13.60	15.27
678 #73	6.22	13.99
678 #71	11.74	13.55
678 #72	35.76	38.46
678 #70	15.09	15.41
678 #69	13.48	13.58
678 #67	23.10	27.35
678 #68	10.63	10.43
678 #63	24.68	27.12
678 #64	16.92	17.13
678#94	21.92	22.84
678 #62	15.67	16.23
678 #10	11.64	12.41
678 #12	10.73	10.00
678 #03	7.31	8.68
678 #65	16.18	17.50
271-9	5.22	8.30
678 #13	4.61	6.49
678 #35	6.98	7.83

678 #87	14.86	13.02
271-5	0.00	0.00
271 -2	11.50	9.99
271-4	4.32	4.53
271 - 3	4.60	3.46
271-16	2.81	3.11
345-13	10.61	9.29
271 - 1	8.45	7.79
345 -25	10.42	10.71
678#104	9.11	9.07
678 107	225.11	223.27
678#111	119.03	119.37
678#108	31.85	31.63
678#109	38.05	38.36
678#110	37.07	37.07
678#112	75.28	75.32
678#15	0.00	0.00
678#52	0.00	0.00
271 -5	0.00	0.00

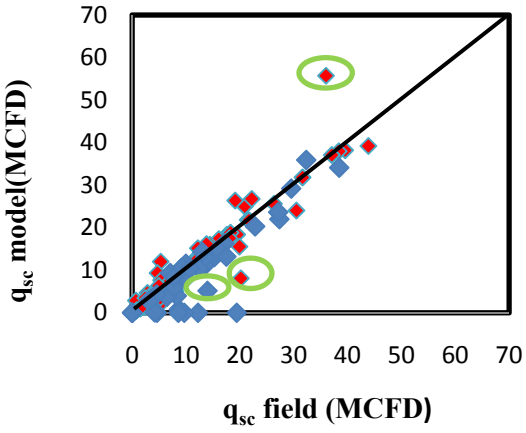

Figure 5 -18a: Cross plot -1 for the entire north section

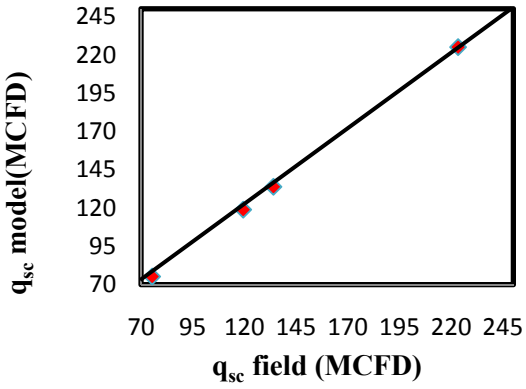

Figure 5-18b: Cross plot-2 for the entire north section

As we can see in Figure 5 - 18a and 5 - 18b, the match between the model predictions and field well flow rates are good. The points lying on the horizontal axis in Figure 5-18a show the wells that are predicted by the model to be shut. There are a few significant outliers which are encircled in green. The deliverability plots of those wells are shown in Figures 5-19, 5-20 and 5-21. The above plots indicate that either the fit is poor or there is an opposite deliverability relationship which made it difficult to get good representative values of P_{shut} and C_{well} for these wells.

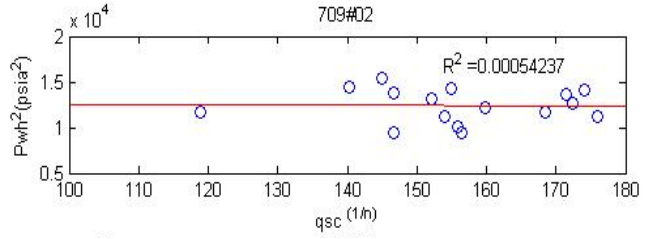

Figure 5-19: 709#02 well deliverability plot

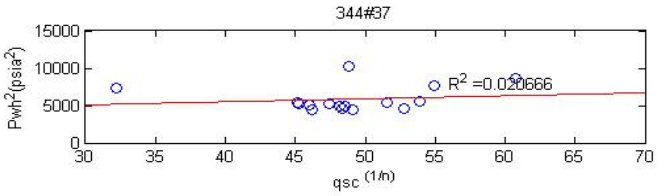

Figure 5-20: 344#37 well deliverability plot

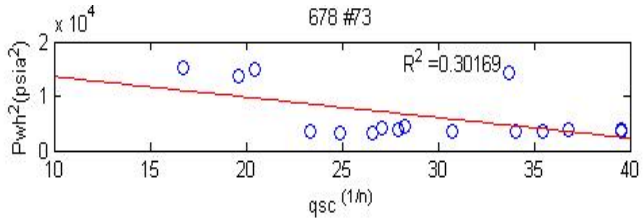

Figure 5-21: 678#73 well deliverability plot

5.5 Modeling with updated IPR information

Based on the results obtained in the preliminary study the next step was to study and analyze the model predictions by using the P_{shut} provided by the operator. The C_{wells} were calculated using the new shut in pressure and the production history of the wells by using equation 5.1. The north section of the network was modeled again with the revised shut in pressures and C_{well}'s to see the adaptability of the network to these new values. Figure 5-22 shows the cross plot comparing field and predicted flow rates after modeling the new case. As we can see we get a good match except for a few outliers. One important thing that has to be observed in Figure 5-24 when compared to Figure 5 - 18a is that the points which were in the horizontal axis have shifted to the vertical axis (circled in blue) in Figure 5 -22. The model predicts the production from these wells to still happen though in reality the wells are not producing anymore. This is due to the fact that the shut in pressure provided by the operator is in the range of 300 psia – 1500 psia while the maximum prevailing pressure at the wellheads in that region is 120 psia and since the difference in the network pressure change is not very high the wells continue to produce as predicted by the model.

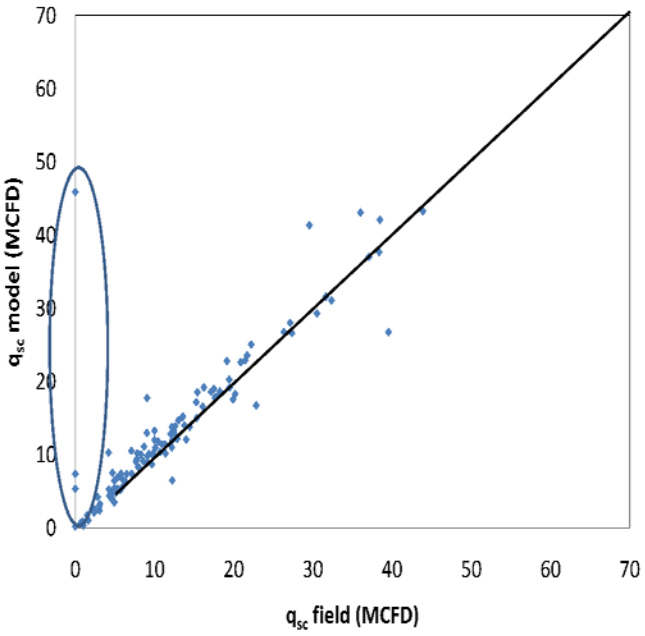

Figure 5-22: Cross plot with revised P_{shut} and C_{well} – North section

5.6 Modeling the Entire Network and History Matching

The C_{well} for the remaining producing wells in the rest of the network was computed using the procedure described in section 5.5. The cross plots showing the model predicted flow rates and the field production data are shown for three different months in Figures 5-23,5-24 & 5 -25. The cross plots cover the entire network in terms of metered producing wells. The model predictions are still good when the analysis was done considering the network as a whole. Wells which did not have deliverability information that is unmetered wells with very small production were represented with a Q_{sc} of 0.001 MCFD in the model as indicated by the operator. The dashed lines in Figures 5-23, 5-24 & 5 -25 represent an allowable bandwidth of 20% between the field flow rates and the model predicted flow rates.

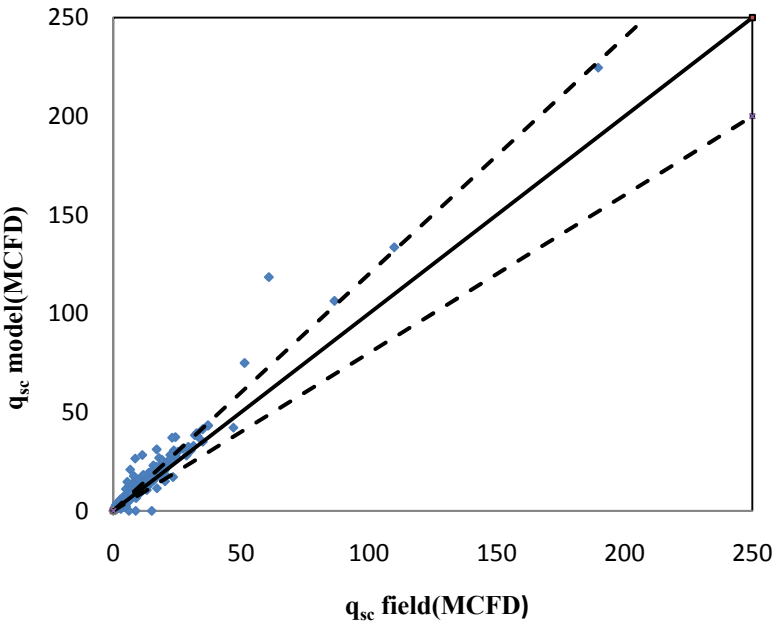

Figure 5 -23: Cross plot total network – April 2008

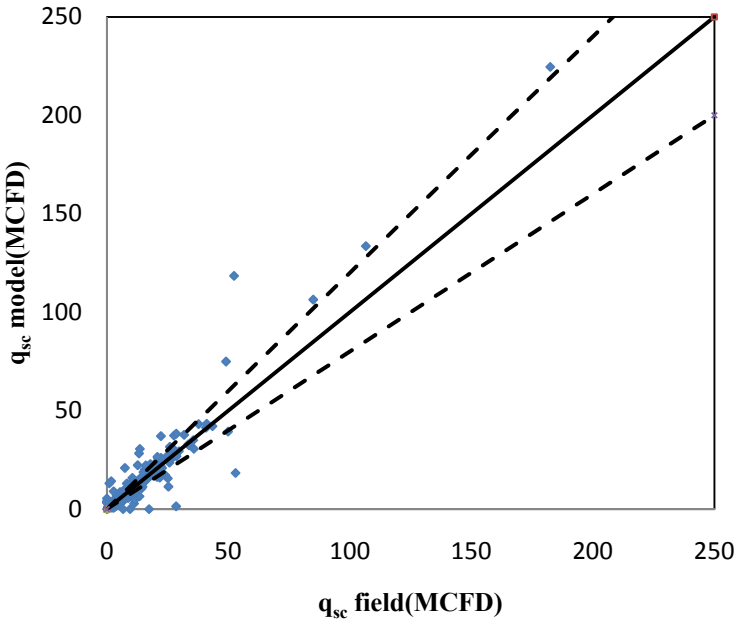

Figure 5 -24: Cross plot total network – May 2008

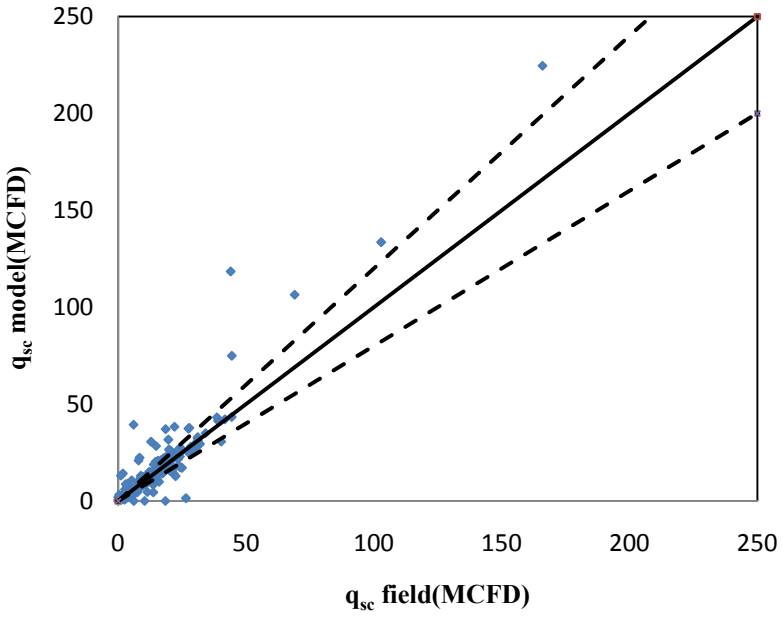

Figure 5 -25: Cross plot total network – July 2008

5.7 Sensitivity Analysis – Compressor suction

A sensitivity analysis was carried out to determine how sensitive the model is with respect to deliverability predictions when different parameters were varied in the model. This is an important aspect in model development and evaluation. Experimenting with different operating parameters as inputs, one can test the behavior of the model under a variety of conditions. This exercise can help in determining the boundaries till which the model can be stretched without compromising the physical meaning of the generated results. In this study, the model was tested by varying the suction pressure of the various compressors located at different points in the network to determine the changes in the deliverability predictions in the entire network. The idea was to see how much loss of system deliverability is realized with lower compression work. The parameter chosen here was suction pressures of the compressors since a particular significance of incorporating compressors in a gas transportation network is to increase the deliverability from the producing wells by lowering the well head pressures. Also, by

lowering suction pressures saving on compressor fuel consumption can be realized. Table 5-4 shows the different cases considered for sensitivity analysis.

Table 5-4: Description of different cases considered for sensitivity analysis – compressor suction

CASE	VARIATION IN SUCTION PRESSURES OF COMPRESSORS
1	5 psig reduction
2	10 psig reduction
3	10 psig increase
4	20 psig increase
5	30 psig increase
6	40 psig increase

Before evaluating the different cases a base case scenario (Fig. 5-26) was modeled with current operating conditions to estimate the total net deliverability. To account for the losses in the system, a gas loss factor of 17% was specified at the wellheads. Out of the four sales points in the network, the sales point present in the middle section of the network was used as the balance node. At the remaining demand locations, a constant demand input was used. The model outputs for the different cases are displayed from Figure 5-27 to 5-32 in terms of total production from the wells and total sales.

RESULTS – BASE CASE

SALES POINTS			
NORTH SECTION	650	MCFD	Specified-Demand
MIDDLE SECTION	3982	MCFD	(Balance Node)
SOUTH SECTION 1	200	MCFD	Specified-Demand
SOUTH SECTION 2	900	MCFD	Specified-Demand
TOTAL SALES	5732	MCFD	

PRODUCTION FROM WELLS		
NORTH SECTION	2088.78	MCFD
MIDDLE SECTION	2390.56	MCFD
SOUTH SECTION	2394.10	MCFD
TOTAL PRODUCTION	6873	MCFD

Figure 5-26: Model output base case

SENSITIVITY ANALYSIS RESULTS – CASE 1

SALES POINTS			
NORTH SECTION	650	MCFD	Specified-Demand
MIDDLE SECTION	3987	MCFD	(Balance Node)
SOUTH SECTION 1	200	MCFD	Specified-Demand
SOUTH SECTION 2	900	MCFD	Specified-Demand
TOTAL SALES	5737	MCFD	

PRODUCTION FROM WELLS		
NORTH SECTION	2088.78	MCFD
MIDDLE SECTION	2395.56	MCFD
SOUTH SECTION	2394.10	MCFD
TOTAL PRODUCTION	6878	MCFD

Figure 5-27: Model output case 1(5 psig uniform suction pressure drop)

SENSITIVITY ANALYSIS RESULTS – CASE 2

SALES POINTS			
NORTH SECTION	650	MCFD	Specified-Demand
MIDDLE SECTION	3990	MCFD	(Balance Node)
SOUTH SECTION	200	MCFD	Specified-Demand
SOUTH SECTION	900	MCFD	Specified-Demand
TOTAL SALES	5740	MCFD	

PRODUCTION FROM WELLS		
NORTH SECTION	2088.78	MCFD
MIDDLE SECTION	2399.56	MCFD
SOUTH SECTION	2394.10	MCFD
TOTAL PRODUCTION	6882	MCFD

Figure 5-28: Model output case 2(10 psig uniform suction pressure drop)

SENSITIVITY ANALYSIS RESULTS – CASE 3

SALES POINTS			
NORTH SECTION	650	MCFD	Specified-Demand
MIDDLE SECTION	3971	MCFD	(Balance Node)
SOUTH SECTION	200	MCFD	Specified-Demand
SOUTH SECTION	900	MCFD	Specified-Demand
TOTAL SALES	5721	MCFD	

PRODUCTION FROM WELLS		
NORTH SECTION	2088.78	MCFD
MIDDLE SECTION	2399.56	MCFD
SOUTH SECTION	2372.10	MCFD
TOTAL PRODUCTION	6860	MCFD

Figure 5-29: Model output case 3(10 psig uniform suction pressure increase)

SENSITIVITY ANALYSIS RESULTS – CASE 4

SALES POINTS			
NORTH SECTION	650	MCFD	Specified-Demand
MIDDLE SECTION	3959	MCFD	(Balance Node)
SOUTH SECTION	200	MCFD	Specified-Demand
SOUTH SECTION	900	MCFD	Specified-Demand
TOTAL SALES	5709	MCFD	

PRODUCTION FROM WELLS		
NORTH SECTION	2087.78	MCFD
MIDDLE SECTION	2397.56	MCFD
SOUTH SECTION	2369.70	MCFD
TOTAL PRODUCTION	6855	MCFD

Figure 5-30: Model output case 4(20 psig uniform suction pressure increase)

SENSITIVITY ANALYSIS RESULTS – CASE 5

SALES POINTS			
NORTH SECTION	650	MCFD	Specified-Demand
MIDDLE SECTION	3945	MCFD	(Balance Node)
SOUTH SECTION	200	MCFD	Specified-Demand
SOUTH SECTION	900	MCFD	Specified-Demand
TOTAL SALES	5695	MCFD	

PRODUCTION FROM WELLS		
NORTH SECTION	2088.78	MCFD
MIDDLE SECTION	2393.10	MCFD
SOUTH SECTION	2356.10	MCFD
TOTAL PRODUCTION	6838	MCFD

Figure 5-31: Model output case 5(30 psig uniform suction pressure increase)

SENSITIVITY ANALYSIS RESULTS – CASE 6

SALES POINTS			
NORTH SECTION	650	MCFD	Specified-Demand
MIDDLE SECTION	3932	MCFD	(Balance Node)
SOUTH SECTION	200	MCFD	Specified-Demand
SOUTH SECTION	900	MCFD	Specified-Demand
TOTAL SALES	5682	MCFD	

PRODUCTION FROM WELLS		
NORTH SECTION	2078.78	MCFD
MIDDLE SECTION	2389.56	MCFD
SOUTH SECTION	2344.10	MCFD
TOTAL PRODUCTION	6812	MCFD

Figure 5-32: Model output case 6(40 psig uniform suction pressure increase)

Table 5-5 summarizes the results of the sensitivity analysis. As we can see from Table 5-5, the production increase or decrease with the suction pressure variations is not significant and is relatively unaffected when compared to the base case scenario. The results are also plotted in Figure 5-33. The shut in pressures used for the wells in the network are high and though there is a change in pressure at the wellheads, the deliverability is much less. This is due to the fact that the well performance constant "C_{well}" (calculated using the shut in pressures provided by the operator) is very small making the change in the deliverability predictions relatively insignificant. Also the usage of high shut in pressures is telling the deliverability model that there is enough energy in the reservoir to transport the gas without much compressor help. The reliability of the model predictions primarily depends on the verification of shut in pressures and deliverability plot shapes.

Table 5-5: Results summary - sensitivity analysis

SCENARIO	TOTAL PRODUCTION(MCFD)	TOTAL SALES(MCFD)
BASE CASE	6873	5732
CASE 1 – 5 PSIG DECREASE	6878	5737
CASE 2 – 10 PSIG DECREASE	6882	5740
CASE 3 – 10 PSIG INCREASE	6860	5721
CASE 4 – 20 PSIG INCREASE	6855	5709
CASE 5 – 30 PSIG INCREASE	6838	5695
CASE 6 – 40 PSIG INCREASE	6812	5682

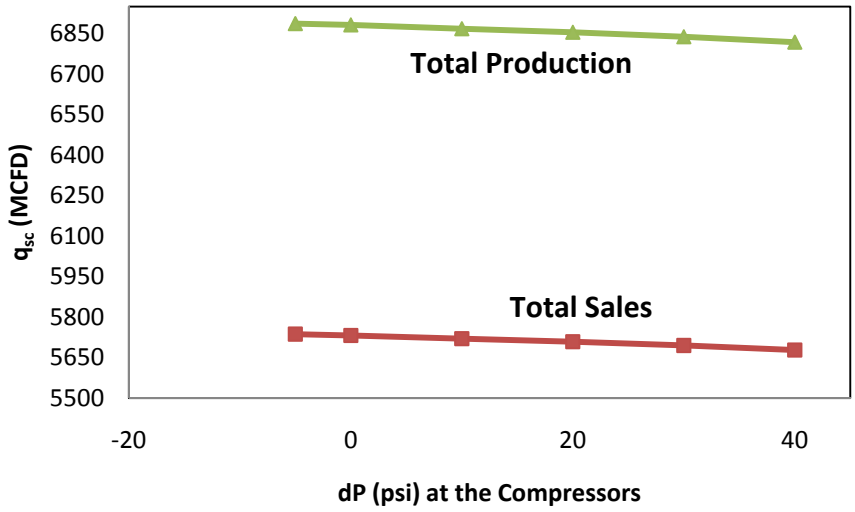

Figure 5- 33: Variation of total production and total sales with changes in compressor suction pressures

5.8 Evaluation of if – then scenarios

Having obtained good history matches, the network model was used for evaluating several scenarios to forecast the total network deliverability of the gas gathering and production system under study by employing a variety of operating conditions. The different cases considered were presented by the operator and are related to the prospective expansion of the network in terms of new well tie-ins and compressor inclusion, provision of tap point, re layout of existing pipeline infrastructure to increase network deliverability. Table 5-6 shows the description of the different if – then scenarios evaluated at different sections of the gas gathering network.

Table 5-6: Description of if – then scenarios

SCENARIO	DESCRIPTION
A	New pipeline addition in the northwest section of the north section of the network
B	Inclusion of a new compressor in the middle section of the network
C	Provision of a new sales point in the south section of the network

SCENARIO A : Inclusion of new compressor in the middle section of the network

On anticipating the possibility of drilling and accommodating high pressure shale wells in this section, a new compressor close to the location of the prospective shale well was planned to be installed to gather gas upstream of this compressor and pump gas directly to the sales point through a separate high pressure discharge line. This separate discharge line was necessary as the shale well was expected to come at very high flow rate and pressure. Figure 5-34 represents the area of interest in the middle section of the network. The location of the shale well and the compressor is shown in Figure 5-34. The purpose of the new compressor is to also increase the production of the wells in the vicinity of the compressor by lowering the well head pressures. Also the compressor will serve to gather gas from any newly added conventional Devonian wells. Without the compressor the well head pressures may go up leading to an eventual decrease in the productivity of the existing wells operating with a stabilized flow regime. To include this new compressor some pipe realignment must be done to the existing pipe configuration to accommodate the high pressure discharge line. Figure 5-35 shows the different modifications that have to be done for the inclusion of the new compressor. Pipe 224 which is a 4” line had to be removed as it is connected to the prospective high pressure discharge line from the new compressor. This separates the group of wells (encircled in black) connected with this pipe from the high pressure line and the production from these wells will flow down the network. A jumper line was introduced to separate one more group of wells connected to the high pressure 6” line and reconnect with the separated group of wells from pipe 224.

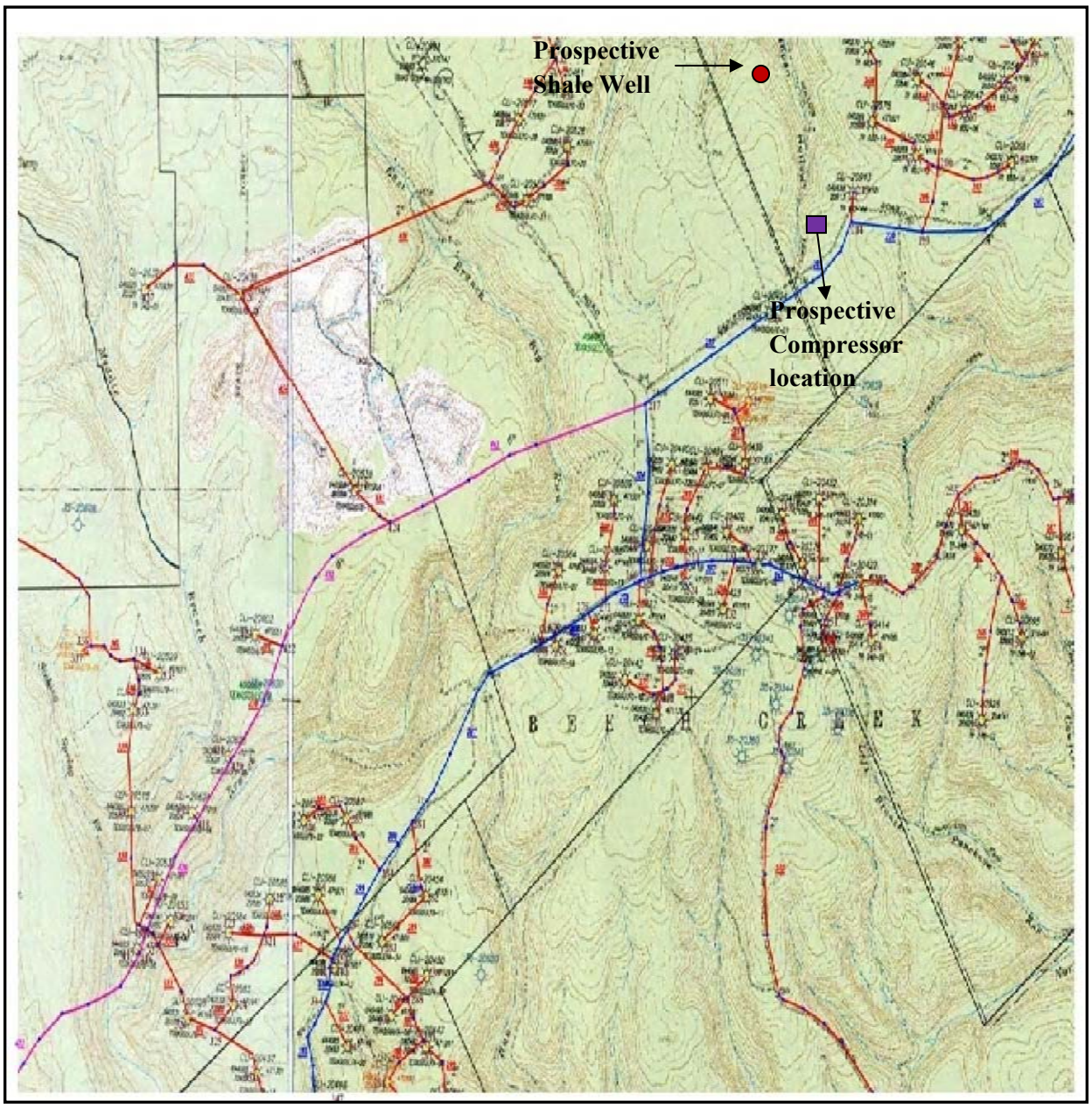

Figure 5-34: Region of interest in the middle section of the network

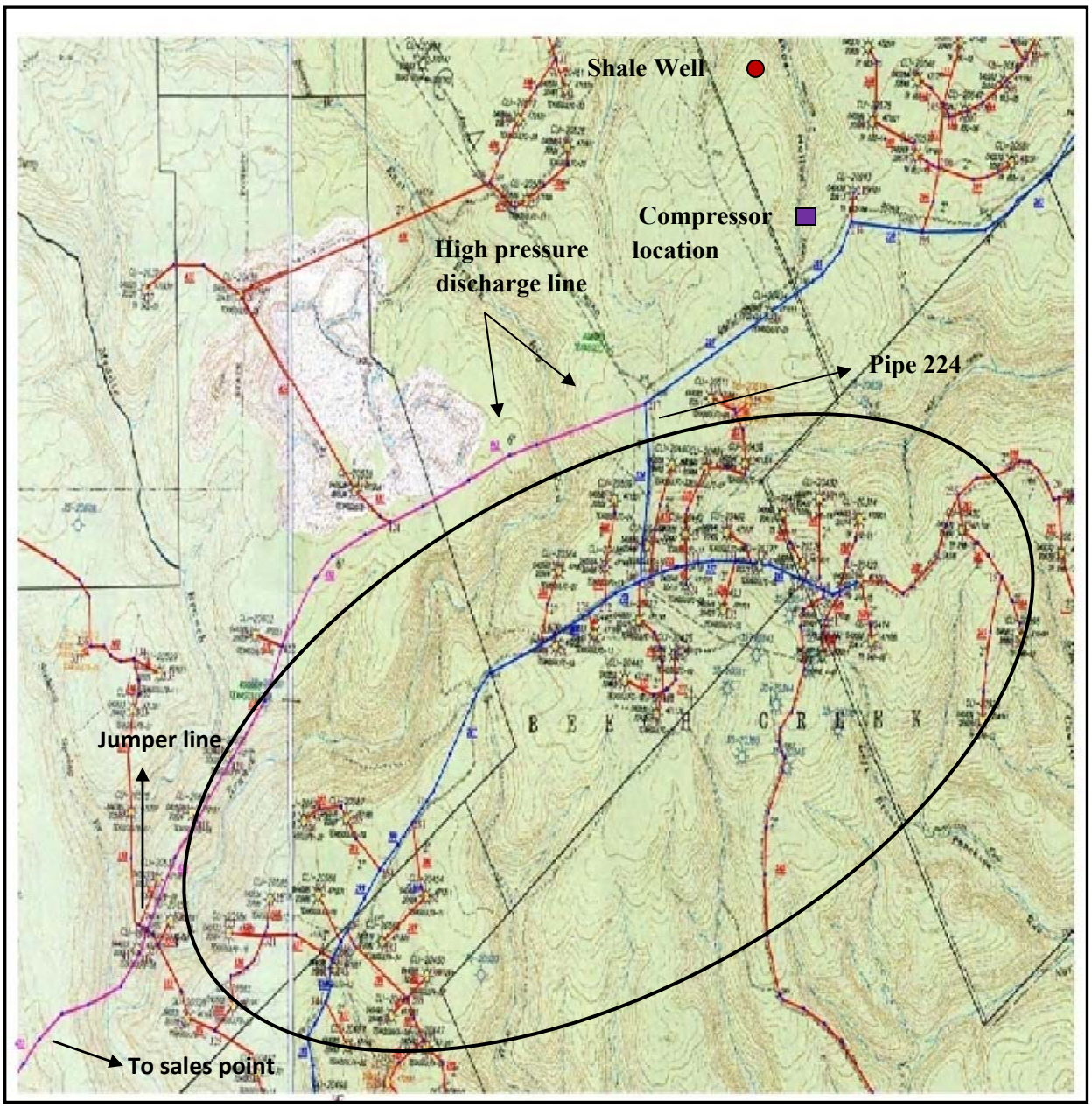

Figure 5-35: Modification in the middle section for inclusion of a new compressor

The facilities and analysis specifications are summarized below.

FACILTIES AND ANALYSIS SPECIFICATIONS:

New compressor
Suction pressure: 35 psig
Discharge pressure: 350 psig

Supplies:
Existing producing wells

Demands:
North section sales point – 650 MCFD
Middle section sales point – balance node
South section - 900 MCFD
South section – 200MCFD

The change in well head pressures of the wells present in the upstream of the new compressor is depicted in Figure 5-36. The blue curve is obtained after joining all the pressure points with the present operating conditions. The red curve is the newly predicted one with the inclusion of the new compressor. As we can see from Figure 5-36, the pressure points in the red curve are slightly below the corresponding pressure points in the blue curve. This indicates that since the well head pressures are lowered with the inclusion of the new compressor, more gas can be expected to flow from the wells in the vicinity of the compressor. The extent of the increase in production will primarily depend on the deliverability information of the producing wells.

The total network deliverability prediction as predicted by the model by using the shut in pressures of the wells obtained from the operator along with the inclusion of the new compressor is 6883 MCFD as shown in Table 5-7. This new value of 6883 MCFD when compared with the total field deliverability of 6873 MCFD before the inclusion of the new compressor as described in Table 5.5 in section 5.7 is not that significant. As described in the sensitivity analysis in section 5.7, the C_{well} of the wells (present in the vicinity of the new compressor) are very less due to the shut in pressures being high and the change in the deliverability prediction is not that pronounced. Though the probable quantification of the deliverability change by the addition of the new compressor wasn't significant, the compressor will still transport gas from the existing producing wells and any new shale well through the separate high pressure discharge line.

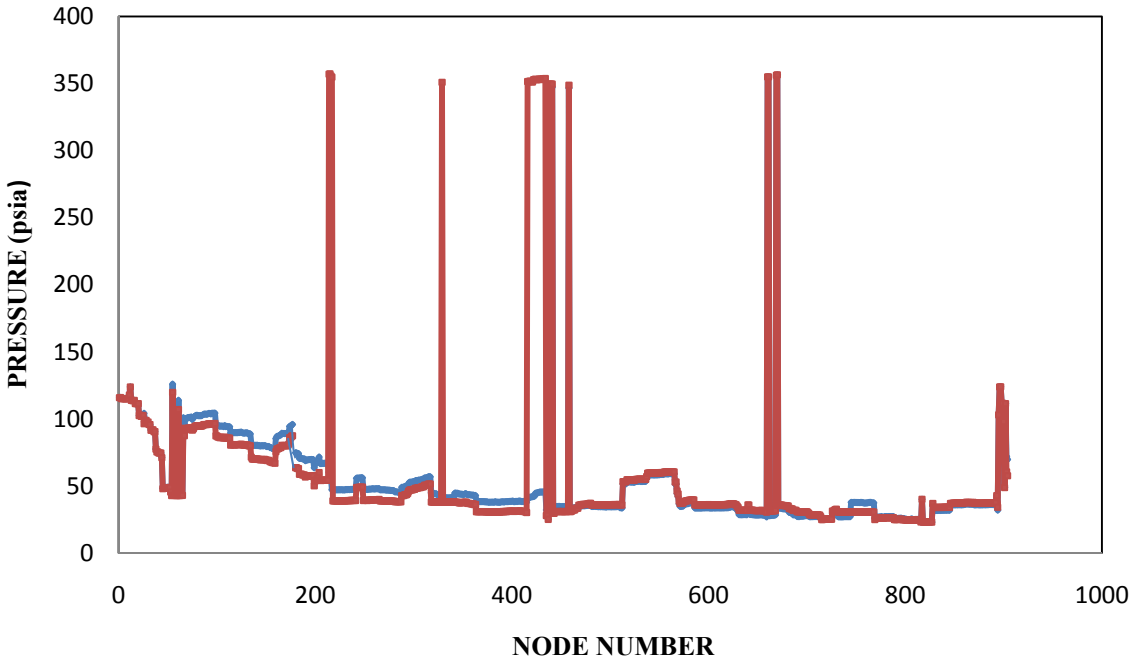

Figure 5-36: Comparison of predicted well head / inter node pressure before and after the inclusion of the new compressor

Table 5-7: Deliverability prediction with the inclusion of the new compressor

SCENARIO A	TOTAL PRODUCTION(MCFD)
Inclusion of new compressor in the middle section	6883

SCENARIO B : New pipeline addition in the northwest section of the network

The north section of the network was a region considered to be having great potential to contribute to existing production in this region as many prospective locations remained unexploited. As part of the new drilling campaign by the operating company, new wells were drilled in this section and tied into the existing network. As a result of the new well tie – ins, the existing well head pressure in this region went up by 70% as these new wells were producing at higher pressures thereby causing a destabilized production regime in the already existing producing wells. Figure 5-37 shows the north section of the network under consideration. As

shown in Figure 5-37, the north section has one infield compressor and one sales point with a peak sales demand of 650 MCFD and also the exact location of the new direct line. The approximate length of the new pipe line is 3.75 miles. The goal of this scenario is to introduce a new direct pipe line from the north section to the sales point.

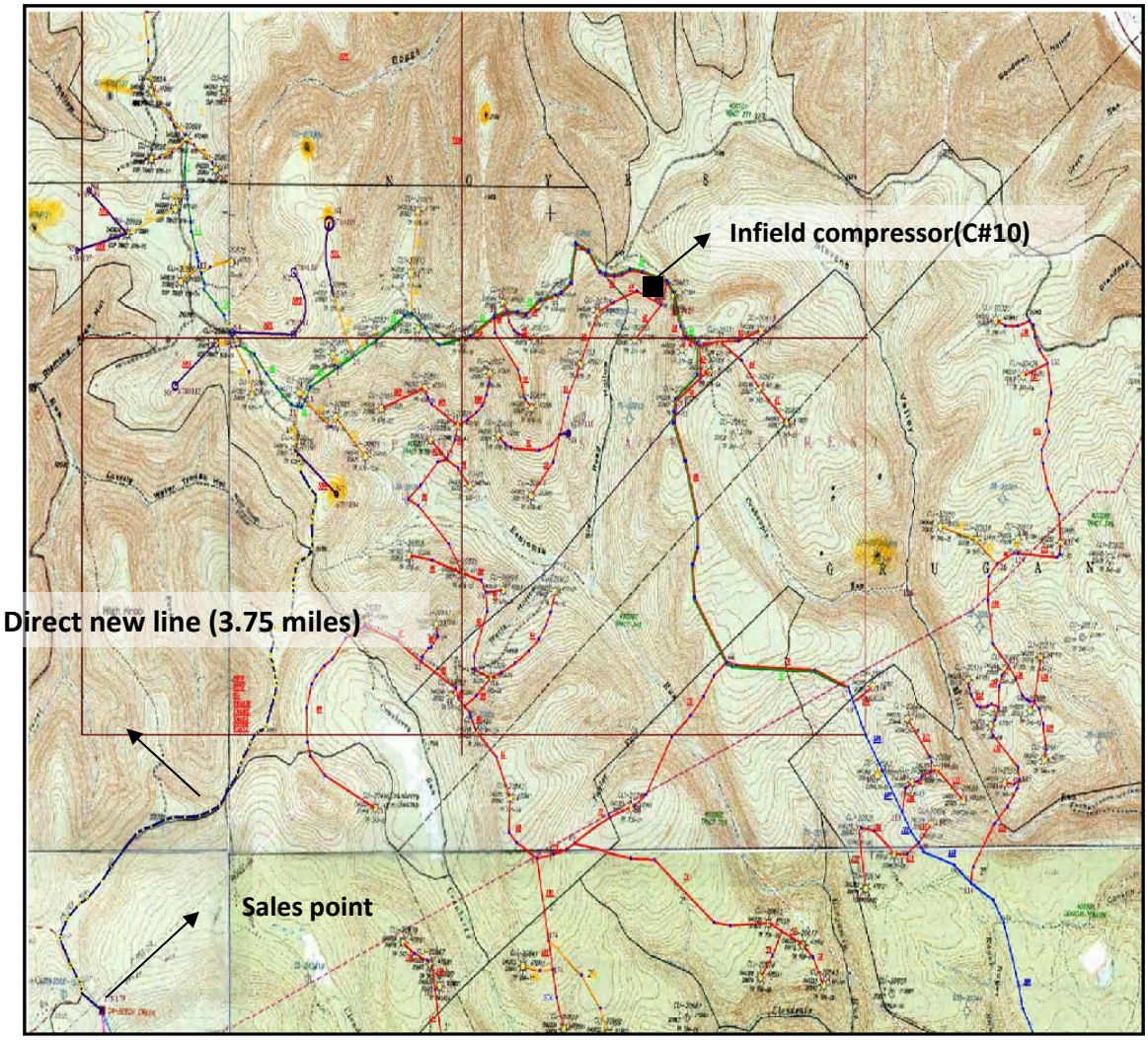

Figure 5-37: Map section showing the prospective direct new line in the North West section of the network

This line could serve as a means to transport most of the gas produced upstream of the infield compressor thus reducing the load on the compressor which could lead to subsequent fuel savings. The new pipe can also lower the existing well head pressures in the region upstream of

the compressor thereby helping the wells to produce more. Therefore the new pipe introduction can have two possible effects. The effect of the new pipeline on the infield compressor was to be studied with increasing pipe diameters of the prospective new line. Three sub scenarios were studied. The first scenario was to evaluate the flow dynamics in the region by assuming a constant suction pressure for the infield compressor, the second scenario is to evaluate by assuming a constant hp for the infield compressor and finally to study the effects without the infield compressor. The results of the analysis of the three sub scenarios are shown in Tables 5-8, 5-9, 5-10.

SCENARIO B1: Results

Table 5-8: Scenario B1– results (constant suction pressure @infield compressor)

	Base Case (no pipe+C#10)	**New pipe i.d**			
		2"	4"	6"	8"
Q new pipe(MCFD)	0	257.78	333.39	337.15	337.61
Infield compressor HP	91.86	66.04	59.12	58.78	58.75
Fuel gas consumption(MCFD)	35.51	25.36	22.70	22.57	22.56
Pre compressor region production(MCFD)	1219	1229.82	1232.41	1232.52	1232.54
Demand at balance node (MCFD)	3783.21	3794.95	3797.61	3797.33	3797.74

We can see from Table 5-8 that the HP of C#10 is getting reduced as the new pipe diameter is increased from 2” to 8”. With the inclusion of the new pipe there is an increase in the production in the pre compressor region, but the increase is very less when compared to the base case production of 3783 MCFD.

SCENARIO B2: Results

Table 5-9: Scenario B2 – results (HP = constant at infield compressor)

	Base Case (no pipe+C#10)	**New pipe i.d (inches)**			
		2"	4"	6"	8"
Q new pipe(MCFD)	0	243.61	305.5	308.41	308.75
Infield compressor HP	91.86	92.47	92.47	92.47	92.47
Fuel gas consumption(MCFD)	35.51	35.51	35.51	35.51	35.51
Pre compressor region production(MCFD)	1219	1235.56	1238.91	1239.06	1239.08
Demand at balance node (MCFD)	3783.21	3800.4	3803.82	3803.97	3803.98

From Table 5-9, we can see that the pre compressor region production is slightly higher for different pipe diameters when compared to scenario B1 case.

SCENARIO B3: Results

Table 5-10: Scenario B3 – results (without infield compressor)

	No pipe/ No C#10	**New pipe i.d (inches)**			
		2”	4”	6”	8”
Q new pipe(MCFD)	0	423.19	612.76	625.85	627.48
C#10 HP	0	0	0	0	0
Fuel gas consumption(MCFD)	0	0	0	0	0
Pre compressor region production(MCFD)	1166.2	1188.91	1199.14	1199.71	1199.78
Demand at balance node (MCFD)	3731.90	3755.67	3764.17	3764.57	3764.62

From Table 5-10, we can see that the volume flowing through the new pipe is significantly greater than the previous two cases. This is because, without the compressor, the gas produced in the region has more tendency to flow through the new pipe line since there is no driving force for the gas to reach the compressor suction. Also the pressures in the pre compressor region are higher without the compressor which explains the slight decrease in the pre compressor production. In all the different scenarios, the deliverability of wells in the pre

compressor region has not been significant with pressure changes and the deliverability information for these wells has to be refined.

This scenario was re evaluated to study the model predictions by using the shut in pressure and well performance constants generated from the back pressure plot instead of the shut in pressures provided by the operator. The north section was modeled alone as a separate entity from the entire network by assuming a constant suction pressure constraint for the infield compressor. The result of the analysis is shown in Table 5-11. From Table 5-11 we can observe that, the total gas available at the sales point because of the direct pipe line is almost twice when compared to the no pipe case. The accuracy of the predicted volume increase due to the new pipeline inclusion is based on the credibility of the P_{shut} and C_{well} generated from the deliverability curves. On the whole, scenario B shows that there will be a definite increase in production and substantial reduction in HP of the infield compressor because of the new pipe line addition though the extent of increase largely depends on the accuracy of the shut in pressures and the well performance constants.

Table 5-11: Results of scenario B re-evaluated with P_{shut} and C_{well} obtained from the backpressure plot (with constant suction pressure @infield compressor)

New pipe dia(inches)	**C#10 HP**	**Demand at balance node (MCFD)**	**Q new pipe(MCFD)**	**Fuel gas consumption (MCFD)**
No pipe	72.2	650	0	27.9
1.5	57.9	805.1	191.3	22.4
2	48.5	916.8	327.2	18.7
3	35.4	1071.1	524.3	13.7
4	30.8	1123.7	594.1	11.9
6	29.1	1143.4	620.7	11.2
8	28.9	1145.8	624.1	11.2

SCENARIO – C: Provision of a new sales point in the south section of the network

The feasibility of the provision of a sales point in the south section of the network in addition to the existing sales points had to be evaluated. Figure 5-38 shows the area of interest in the south section of the network for this particular scenario and the location of the tap point and the infield compressor. This sales point had to be located near a distribution trunk line which was running close to it. This tap point is located near a 4" line which forms as the suction line of the infield compressor. The idea was to see how much gas could be transferred to this main trunk line by providing this tap point. A survey of the existing pressures prevailing in the region close to this tap point was done. The pressures at the various well nodes /internodes were found to be in the range of 20 psia – 25 psia. It was concluded that it is not possible to provide a tap point at this location since there must be a high pressure prevailing in the region to transfer the gas from the 4" line through the tap point into the main trunk line system. This could probably be done by locating a booster compressor close to the tap point or by-passing the infield compressor or by connecting newly drilled wells into the system in the concerned region which would raise the well head pressure in the locality thereby increasing the overall system pressure in that region.

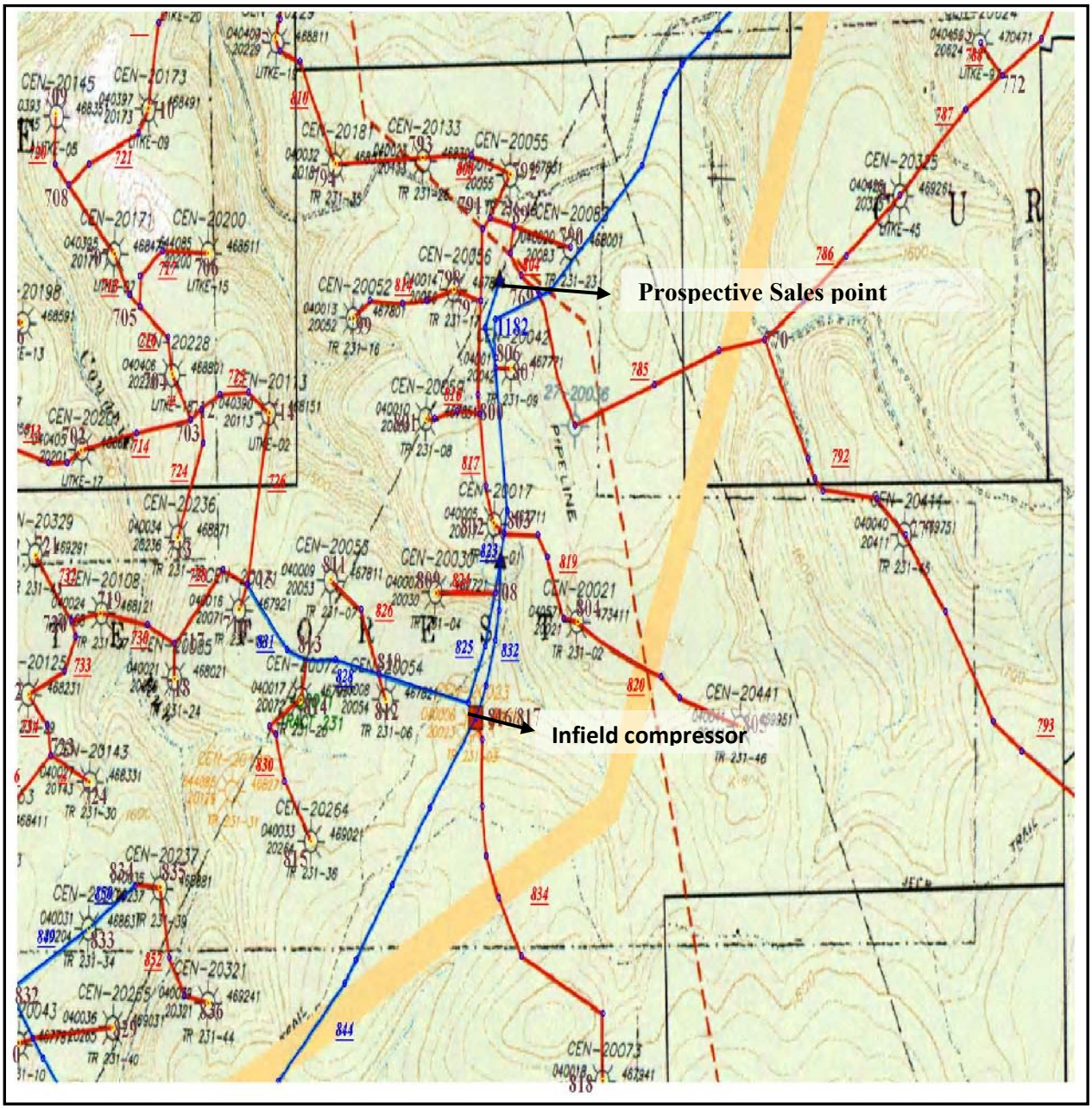

Figure 5-38: The region of interest for the provision of sales point in the south section of the network

Chapter 6

CONCLUDING REMARKS

The integrated steady state model developed in this study was effective in predicting the well deliverabilities by the inclusion of the well deliverability equation embedded into the surface gas network model based on the good history matches obtained. A more realistic modeling was done by using the integrated model to predict the well production in addition to the nodal pressures. Though the reservoir parameters were unknown to compute the deliverability information, the method described to generate the shut in pressures and the well deliverability constants from the well inflow deliverability plot proved to be useful to generate the necessary information which served as vital inputs to the model. The accuracy of this method largely depends on how far the production history of a particular well could be trusted as a level of approximation had to be done to generate the shut in pressure for those particular wells having an erratic production history.

This model is a simple, yet useful, decision making tool to analyze a gas gathering system for understanding the flow dynamics in relation to prospective modifications in connection with network expansion. However the accuracy of the deliverability predictions depends on the shut in pressure and the well deliverability constant (C_{well}).

The sensitivity analysis carried out showed that the flow predictions are quite insignificant to changes in network pressure as the C_{well}'s are nearly zero which makes the inflow performance curve a near vertical line which means the well deliverability is basically unaffected by the prevailing well head pressure. By accounting for compressor fuel consumption and well head losses, the model can help in sizing compressors for a given compression ratio and capturing unknown physical losses respectively. Though this model was customized to the gas gathering system under study, it could be extended to deal with different gas formations with appropriate changes. This model could be further diversified by including modules to account for facilities

like regulators, valves, underground gas storage etc with special emphasis on multiphase flow in pipes.

The shut in pressures provided by the operating company were empirically calculated and using them as inputs for all the producing wells decreased the well performance constant thereby decreasing the total productivity of the wells. A method to cross check these shut in pressures can be done by putting the wells under test to gather the necessary information. Though it is not practically feasible to shut in each and every producing well, a group of wells in the different sections of the network can be chosen to represent the production behavior in that particular region and tests can be conducted to monitor the flow and pressure changes by installing back pressure regulators at the well heads. The data collected from these wells can be used to calibrate the well performance constants and the shut in pressures. The model can be further enhanced by including tubing performance relationship to give more accurate deliverability prediction if the tubing and completion data for the wells are available.

REFERENCES

1. Aina, I., " Steady State and Transient Flow Studies in Natural Gas Pipelines", M.S Thesis, The Pennsylvania State University, University Park, PA, USA, 2006.
2. Ayala, L.F., PNG 530 Class Notes, The Pennsylvania State University, University Park, PA, Spring 2008.
3. Baldwin, J.O., "Prediction of Deliverability from a Multi - Well Gas Reservoir" SPE Proceedings –55th Annual Fall Technical Conference and Exhibition, Dallas, TX, September 21 - 24, 1980.
4. Carrillo S., "A Compositional Network Pipeline Model as a Tool for Decision Making", M.S. Thesis, The Pennsylvania State University, University Park, PA, USA,1999.
5. Chaudhry, A.U., "Gas Well Testing Handbook", Gulf Professional Publishing, MA, p 140 -167, 2003.
6. Dempsey, J.R *et al.*, " An efficient Model for Evaluating Gas Field Gathering System Design", Journal of Petroleum Technology, v 23, p 1067 – 1073, 1971.
7. Donohue, D.A.T. and Ertekin, T., "Gas Well Testing Theory, Practice & Regulation", IHRDC, Boston, p 6 – 22, 1982.
8. Dranchuk, P.M. and Abou-Kassem, J.H., "Calculation of Z Factors for Natural Gases Using Equations of State," Journal of Canadian Petroleum Technology, July-September, p 34-36, 1975.
9. Guo, B. and Ghalambhor, A., "Natural Gas Engineering Handbook", Gulf publishing company, TX, p 81 – 91, 2005.
10. Hepguler,G. *et al.*, "Application of a Field Surface & Production Network Simulator Integrated With a Reservoir Simulator" SPE Proceedings – Symposium on Reservoir Simulation, Dallas, TX , June 8-11, p 285 -286, 1997.

11. Holst, R. *et al.,* "Computer Optimization of Large Gas Reservoirs with Complex Gathering Systems" Proceedings – SPE Annual Technical Conference and Exhibition,Houston,TX,October 3 -6, 1999.
12. Ikoku,C.U.,"Natural Gas Reservoir Engineering", Krieger Publishing Company, FL, p 279 -295, 1992.
13. Kelkar,M., "Natural Gas Production Engineering", PennWell Corporation, OK, 2008.
14. Krishnamurthy, J. " Performance Analysis of Natural Gas Gathering and Production Systems", M.S. Thesis, The Pennsylvania State University, University Park, PA, USA, 2008.
15. Kumar, S., "Gas Production Engineering ", Gulf publishing company, v. 4. TX, p 394 – 450, 1987.
16. Lee, A.L., Gonzales, M.H., and Eakin, B.E., "The Viscosity of Natural Gas" Journal of Petroleum Technology, August, p 997 – 1000, 1966.
17. Marsh, J., Kenny, J., "Wildcat Hills Gas Gathering System Case Studies: An Integrated Approach From Reservoir Development to Sales Pipeline Delivery" SPE Proceedings – Gas Technology Symposium , Calgary, Alberta, Canada, 30th April – 2nd May, p 571 – 583, 2002.
18. Matthews, C.S., and Russell, D. G., "Pressure Buildup and Flow tests in Wells", SPE Monograph Series, No.1, SPE, Dallas, Texas, 1967.
19. Menon, E.,"Gas Pipeline Hydraulics", Taylor and Francis Group, FL, p 31 – 80, 2005.
20. Mogensen, A.C. *et al.*, "Application of integrated reservoir simulation and pipeline network modeling software to the Sexsmith gas – condensate field" SPE Proceedings – Gas Technology Symposium, Calgary,Alberta,Canada, March 15 – 18, p291 -297, 1998.
21. Mokhatab, S. *et al.*, "Handbook of Natural Gas Transmission and Processing", Gulf Professional Publishing, MA, p 401 – 408, 2006.
22. Nagoo, A. " Analysis of steady and quasi steady flows in complex pipe topology", M.S. Thesis, The Pennsylvania State University, University Park, PA, USA, 2003.

23. Schellhardt, M.A., and Rawlins, E.L., "Back Pressure Data on Natural Gas Wells and Their Application to Production Practice", United States Bureau of Mines, Monograph 7, 1936.
24. Stevenson, B.K., O'Shea, C.D., " Case Study: Modeling of a Large-Scale Tight Gas Gathering System" SPE Proceedings – Gas Technology Symposium,Calgary, Alberta, Canada, May 15 -18, p 244 -248, 2006.
25. Startzman,R.A. *et al.*, "Computer Combines Offshore Facilities and Reservoir Forecasts", Petroleum Engineer International, v 49, n 5, p 65, 68, 70, 74, 1977.
26. Stoner, M.A., "Steady – State Analysis of Gas Production, Transmission and Distribution Systems" Journal of Petroleum Technology, 1969.
27. Tingas, J. *et al*., "Integrated Reservoir and Surface Network Simulation in Reservoir Management of Southern North Sea Gas Reservoirs" SPE Proceedings – European Petroleum Conference, v 2, The Hague, Netherlands, October 20 – 22, p 51 – 62, 1998.
28. Trick, M.D.," A Different Approach to Coupling a Reservoir Simulator with a Surface Facilities Model" SPE Proceedings – Gas Technology Symposium, Calgary,Alberta,Canada, March 15 – 18, p 285 – 290, 1998.
29. US Department of Energy (US DOE), 2009,"About US Natural Gas Pipelines – Transporting Natural Gas", http://www.eia.doe.gov/pub/oil_gas/natural_gas/analysis_publications/ngpipeline/, last accessed: June 20, 2009.

Appendix A

Theoretical Compressor Equation

The compression process can be basically characterized into 3 types based on the thermodynamics of the pressure and volume changes taking place during the process. They are

1. Isothermal compression
2. Isentropic compression
3. Polytropic compression

The isothermal compression case is the ideal case where the work or the HP required for compression is the minimum when compared to the other two compression process as the temperature is kept constant during the compression process but in reality isothermal compression is difficult to achieve. The isentropic or the reversible adiabatic compression is the process where the gas behaves as an ideal gas with no friction losses and no heat transfer takes place during the compression/expansion process. Positive displacement compressors are designed assuming an isentropic behavior. The pressure and volume changes during an isentropic compression is given by

$$\boldsymbol{P_1 {V_1}^k = P_2 {V_2}^k = constant} \quad \boldsymbol{----(1)}$$

where 1, 2 refer to the initial and final states of compressed gas and k is the isentropic exponent which is equal to the ratio of the specific heat at constant pressure and specific heat at constant volume

$$\boldsymbol{k = \frac{C_p}{C_v}}$$

Invoking the first law of Thermodynamics, the work done on a unit mass of fluid being compressed under steady state conditions yields the following expression:

$$\boldsymbol{w = \int_{Psuction}^{Pdischarge} (Vdp + \frac{\Delta v^2}{2g_c} + \Delta z(\frac{g}{g_c}) + l_w) - - - - - (2)}$$

where

w = work done by the compressor on the gas, ft – lbf/lbm

V = volume of gas, ft3/lbm

p = pressure, psi

v = gas velocity, ft/sec

z = elevation, ft

l_w = work lost due to friction and irreversibility's, ft –lbf/lbm

Neglecting changes in potential and kinetic energies and assuming the process is frictionless and incorporating equation 1 in equation 2, the integrated form of the equation which gives the ideal horse power (I.H.P) in a consistent set of units is given as

$$\boldsymbol{\frac{IHP}{Qs} = 3.0303 P_{SC} (\frac{Tav}{Tsc})(\frac{k}{k-1})\left(\frac{P_{discharge}}{P_{suction}}^{(k-1)/k} - 1\right) - - - - - (3)}$$

Equation 3 represents the HP requirement for an isentropic compression process for an ideal gas, which assumes adiabatic and reversible conditions. For real gases, equation 3 can be modified by incorporating a Z factor ratio. For general compression processes, non-adiabatic conditions are represented by exchanging the adiabatic exponent "k" with the polytropic coefficient "n". These modifications yield:

$$\frac{IHP}{Qs} = 3.0303P_{SC}\left(\frac{Tav}{Tsc}\right)\left(\frac{n}{n-1}\right)\left(\frac{P_{discharge}}{P_{suction}}^{(n-1)/n} - 1\right)\left(\frac{Z_1}{Z_{SC}}\right) - - - - - (4)$$

Equation 4 implicitly assumes that compression is taking place in a single stage. If more than 1 stage is used, this equation can be further modified to account for it. In multistage compression, optimum operation requires for each stage to be carried out with the same compression ratio. Assuming that intercooling takes place between each stage, equation (4) can be expressed as:

$$\frac{IHP}{Qs} = 3.0303P_{SC}\ \alpha\left(\frac{Tav}{Tsc}\right)\left(\frac{n}{n-1}\right)\left(\frac{P_{discharge}}{P_{suction}}^{(n-1)/(\alpha \cdot n)} - 1\right)\left(\frac{Z_1}{Z_{SC}}\right) - - - - - (5)$$

where, α = number of stages. In order to account for the irreversibilites of the process, we calculate actual HP (BHP) as a function of the ideal HP (IHP) by the introduction of the compressor efficiency(η). Therefore:

$$BHP = \frac{IHP}{\eta} - - - - - (6)$$

Therefore, by inspection of equation 5 and 6, compressor performance can be expressed as:

$$\frac{HP}{Q_s} = (K_1 R^{K_3} - K_2) \text{ ---------- } (7)$$

where:

HP = Power in horsepower units

R = total compression ratio

Q_s =Gas Flow rate at standard conditions (MMSCFD)

Z_1 = Compressibility factor at suction conditions

Z_{SC} = Compressibility factor at standard conditions

K_1, K_2, K_3 - compressor coefficients

where:

$K_1 = K_2 = \frac{3.03P_{SC}}{\eta}\alpha\left(\frac{n}{n-1}\right)(Z_1/Z_{SC})(\frac{T_{av}}{Tsc})$

$K_3 = (n-1)/(\alpha \cdot n)$

where

P_{SC} = Standard pressure = 14.7 psia

η = Compressor efficiency

n = polytropic exponent

α = number of stages.

Tav = Average temperature, R

Tsc = Standard temperature = 520 R

Appendix B

Pipe flow equation and friction factor models

Pipe flow equation	Friction factor model
General	Modified Colebrook – White friction factor $\frac{1}{\sqrt{f}} = -2log10(\frac{0.0000316}{3.7} + \frac{2.825}{5331726\sqrt{f}})$
Weymouth	$f = \frac{0.008}{D^{\frac{1}{3}}}$
Panhandle A	$f = \frac{0.019231}{(\frac{Q_{sc}\gamma_g}{D})^{0.1461}}$
Panhandle B	$f = \frac{0.003586}{(\frac{Q_{sc}\gamma_g}{D})^{0.03922}}$